2019

Chemical Composition of Preclassic-Period Maya Slips: Analysis and Interpretation of Flores Waxy Ware and Paso Caballo Waxy Ware Sherds from Holtun, Guatemala Using pXRF Spectrometry

Anna Kebler
University of Central Florida

CHEMICAL COMPOSITION OF PRECLASSIC-PERIOD MAYA SLIPS: ANALYSIS AND INTERPRETATION OF FLORES WAXY WARE AND PASO CABALLO WAXY WARE SHERDS FROM HOLTUN, GUATEMALA USING PXRF SPECTROMETRY

by

ANNA E. KEBLER
B.A. University of New Mexico, 2016

A thesis submitted in partial fulfillment of the requirements
for the degree of Master of Arts
in the Department of Anthropology
in the College of Sciences
at the University of Central Florida
Orlando, Florida

Spring Term
2019

ABSTRACT

Slip, a fluid suspension of clay that is applied to the surface of a piece of ceramic, allows for increased control over the functional and aesthetic properties of a finished vessel. The potter can select a slip to provide a more appealing color, texture, and/or luster to the vessel's surface, while maintaining the favorable functional qualities of the paste. Though slip color has long been used as an attribute for classification in the Maya lowlands, only recently have the raw materials of slips been used to inform studies of production and exchange, with much of this work using Late and Terminal Classic-period ceramics and analysis techniques that require taking small samples of each ceramic to be analyzed. Such studies present an incomplete picture of Maya slips, since they only include later ceramics and exclude vessels from which samples cannot be taken. This thesis broadens our understanding of Maya slips by 1) establishing portable x-ray fluorescence (pXRF) spectrometry as a nondestructive analysis technique that can be used to chemically characterize slips on a wide range of sherd sizes and whole vessels, and 2) determining the chemical compositions of red, cream, and black slips on Middle and Late Preclassic-period ceramic sherds excavated in 2017 from Holtun, Guatemala. The data produced through pXRF spectrometry revealed that red slips were chemically distinct from the other two colors, while white and black slips were chemically indistinct. Iron, zinc, molybdenum, tin, and antimony concentrations were the principal determinants of compositional groups. These results indicate that these elements are of primary interest in sourcing the clays used to make the slips, and trends in the chemical composition of each color have the potential to reveal much about Maya potters' processes and standardization in slip production.

Keywords: ceramic slip, pXRF, Preclassic, chemical composition

ACKNOWLEDGEMENTS

First, I would like to thank my advisor, Dr. Michael Callaghan, for his dedication, support, and patience throughout my time at UCF. I would like to thank Dr. Bridgette Kovacevich, and Dr. Sarah Barber. Not only have they generously provided their time and feedback as members of my thesis committee, but I have become a better archaeologist and scientific writer as a result of their classes. I would also like to thank Dr. John Walker for joining my committee last minute to fill-in for the defense. I would like to thank all the members of the 2017 Holtun Archaeological Project. This thesis would not have been possible without all of their hard work. Last but not least, I want to thank my family, who have (sometimes) willing listened to me talk about the ancient Maya and ceramic analysis for hours. This exemplifies the unconditional love, continuous support, and near-bottomless patience my parents and sister have provided over the years. I would not have accomplished what I have without them.

TABLE OF CONTENTS

LIST OF FIGURES

LIST OF TABLES

LIST OF ABBREVIATIONS

μA: microampere

Elements:

As: arsenic

Ba: barium

Ca: calcium

Co: cobalt

Cr: chromium

Cu: copper

Fe: iron

Mn: manganese

Mo: Molybdenum

Nb: niobium

Ni: nickel

Rb: rubidium

Rh: rhodium

Sb: antimony

Sn: tin

Sr: strontium

Th: thorium

Ti: titanium

U: uranium

Y: yttrium

Zn: zinc

Zr: zirconium

eV: electronvolt

INAA: instrumental neutron activation analysis

keV: kiloelectronvolt

LA-ICP-MS: laser ablation-inductively coupled plasma-mass spectrometry

MNI: minimum number of individuals

MNV: minimum number of vessels

n.d.: no date

ppb: parts-per-billion

ppm: parts-per-million

pXRF: portable x-ray fluorescence

ROI: region of interest

SDD: Silicon Drift Detector

vs: versus

XRF: x-ray fluorescence

CHAPTER 1: INTRODUCTION

Since first being used for archaeological purposes in the 1960s, x-ray fluorescence (XRF) has become a particularly popular method of qualitatively and quantitatively assessing the chemical compositions of archaeological and historical materials (Speakman et al. 2011; Shackley 2012a). Its popularity in investigating such materials stems from several key advantages: non-destructive sampling, minimal sample preparation, speed of analysis, easiness of use, and cost-effectiveness per sample relative to other methods of analysis (Shackley 2012b). As the name suggests, portable XRF (pXRF) spectrometry has the added advantage of portability, allowing for *in situ* analysis.

While ceramic objects, be they sherds for who vessels, remain one of the most numerous finds at many archaeological sites, the applications of pXRF spectrometry to the study of archaeological ceramics have been limited when compared to other materials. Archaeologists have raised concerns about the heterogeneity of ceramic composition as a result of low firing temperatures (compared to those at which igneous and metamorphic rock, as well as man-made glass) are formed, the depth the x-ray penetrates, and the effects of human behavior on their creation (Shackley 2012b; Lirtzis and Zachaias 2012; Shugar and Mass 2012). However, these concerns do not mean pXRF spectrometry cannot be used to successfully qualitatively or even quantitatively characterize the chemical compositions of archaeological ceramics; we simply need to evaluate what parts of ceramics are best-suited to pXRF analysis. pXRF spectrometry is a useful non-destructive test for analyzing the chemical composition of slips, and the produced data indicate early standardization of different color slip recipes.

Slips, Standardization, and the Preclassic Maya

As pXRF is best applied as a technique for surface analysis (Liritzis and Zachaias 2012), in the realm of ceramics it is most suitable to paints, glazes, and slips used to decorate and finish the surfaces of ceramics. This thesis concerns ceramic slips. In pottery, a slip is a fluid suspension of clay that is applied to the surface of a piece of ceramic. The use of slip grants the potter increased control over the functional and aesthetic properties of the finished vessel (Shepard 1956; Rice 1987). The potter can select a slip to provide a more appealing color, texture, and/or luster to a vessel's surface, while maintaining the favorable qualities of the paste. In areas where it is used, including the Maya lowlands, slip provides the archaeologist with an important attribute for classification, as well as material for the study of ceramic production and distribution. Its importance increases in areas were glazes were not developed or were unattainable due to low-firing temperatures, or in time-periods were painted decorations on ceramics were minimal or non-existent. Both of these conditions apply to the Preclassic-period Maya lowlands, where slip constituted the main form of surface decorations that was chemically distinct from the paste.

A principal attribute used in many classifications schemes is slip color (Rice 2013; Bill 2013). This is demonstrated by the number of type names referencing the slip color. In the Pre-Mamom- through Late Classic-period Maya lowlands alone, we see type names such as K'atun Red, Joventud Red, Sierra Red, Dos Hermanos Red and Tinaja Red, all referring to red-slipped ceramics (Adams 1971; Callaghan and Nievens de Estrada 2016; Gifford 1976; Kosakowsky 1987; Sabloff 1975). While other ceramic attributes – such as paste, temper, and vessel form – figure prominently in type descriptions, it is the presence of slip and its color that have come to signify the type overall.

With such privilege given to slip in classifications and its importance in the finishing and decorating of Preclassic-period Maya ceramics, one would expect that slip has been subject to much research. Yet only recently have the raw materials of slips been used to inform studies of production and exchange in the Maya area. Leslie G. Cecil and Hector Neff (2006; see also Neff 2003; Cecil 2013) have evaluated the chemical compositions of slips of Postclassic-period Maya ceramics. Their research has shed light on trading patterns as well as technological styles in pottery manufacture and its relationship to socio-political identity among the antagonistic Itzá and Kowoj groups. The conclusions reached by Cecil and Neff demonstrate that the chemical compositions of slip can tell us much about pottery manufacture – namely the choice and procurement of raw materials for differing slip colors – and trade, as well as potentially adding to knowledge about broader economic, social and political trends among the ancient Maya.

When considering the Preclassic period in particular, the distribution of potentially variable slip recipes can also indicate specialization and standardization in ceramic production, as well as increasing social stratification. Rice (1981) proposes that variability and standardization are opposites. She hypothesizes that minimal variation in ceramic attributes, such as decoration and color, result from "an increasingly narrow concept or standard, on the part of manufactures and buyers alike, of what constitutes an acceptable ceramic vessel in any category" and from "increasing skill of potters in achieving that standard" (Rice 1981:222). At the first stage of her model, in which a society is largely egalitarian and pottery production occurs in many households, "more or less random variations [in ceramic attributes] are likely to occur, reflecting individual differences in raw-material sources and/or methods of production" and, as a result, "there should be small (e.g. household) concentrations of similar attributes, not an even distribution of these traits throughout the site" (Rice 1981). Previous research on ceramic pastes

of Middle Preclassic-period sherds from Holtun has suggested that this is not the case. Instead, "the correlation between paste composition and other variables hint at the possibility that few people may have been involved in the production of specific types and wares, and that these few people were making the same choices over and over again" in what could possibly be an instance of "very low level [sic] specialization and incipient standardization in the Middle Preclassic period" (Callaghan et al. 2017:344).

Rice (1981) does not discuss slip recipes in outlining her theoretical model, but does note that paste recipes become increasing similar with increasing standardization. It is reasonable to think that slip recipes would also become more standardized to achieve the desired effects in terms of color, texture, and practical advantages. Therefore, little variation in the chemical composition of slip could point to increasing specialization and standardization. This would support the conclusions drawn from the pastes of Middle Preclassic-period ceramics from Holtun.

Significance

The implications and successes seen by Cecil and Neff highlight the need for further research on slips, including those that have yet to be studied. Scholars are only beginning to determine the chemical compositions and potential procurement areas for Postclassic-period Maya slips, and no research has been done on Preclassic-period Maya slips. As such, the purpose of this thesis is two-fold. First, it is a methodological study of abilities of pXRF spectrometry as a tool for the analysis of ceramic slip. Second, it presents the findings of the chemical composition of Middle and Late Preclassic-period red, white, and black slips found on ceramics excavated during the 2017 field season of the Holtun Archaeological Project.

For the methodological goal, the research question is: How successful is pXRF spectrometry in determining the composition of surface finishes on ceramics? A clean break (a cross-section of slip, paste, and interaction zones broken after excavation and cleaning to prevent contamination from use or deposition), the exterior slipped surface, and the interior slipped surface were analyzed under the same analysis conditions. Using statistical analyses to compare the mean data for the concentrations of each element obtained from clean breaks and slipped surfaces allowed for the assessment of whether pXRF spectrometry could be isolated to the slip alone or was extending into the underlying paste. Comparisons of the slipped surfaces and clean breaks revealed that pXRF analysis was largely able to distinguish between the slip alone and a combination of the slip and the underlying paste, except for a few heavy elements that have a higher depth of penetration of the x-ray beam. Semi-quantitative and qualitative data were produced, and the latter revealed compositional differences between slips. This supports the hypothesis that pXRF would be able to distinguish differences in the chemical compositions of slips.

The second research question is: How do the chemical compositions of different slip colors vary across time and space at Holtun? In other words, how does chemical composition of a given color of slip differ between a) slips of different colors, b) the Middle and Late Preclassic type: varieties of each slip color and c) for slipped sherds excavated from different architectural groups. pXRF spectrometry revealed two distinct compositional groups: one consisting of red-slipped sherds and one consisting of cream- and black-slipped sherds. No chemical distinctions were seen between type: varieties of the same color, indicating no significance variation the composition of a slip of a given color between the Middle and Late Preclassic-periods. Similarly, no variation was seen in chemical compositions of slips of a given color based on where sherds

were excavated. These results supported the hypotheses that there would be compositional differences between slip colors and that there would not be compositional differences corresponding to the architectural group where a sherd was excavated. However, the hypothesis that there would be observable differences between Middle and Late Preclassic-period type: varieties of each color was not supported.

Previous research on the chemical compositions of ceramic pastes from Holtun suggests that Middle Preclassic-period slipped serving ware was locally made, and that there was variability in paste recipes for different slipped type: varieties (Callaghan et al. 2017). In addition to the variability between the paste recipes for different type: varieties, Middle Preclassic-period potters at Holtun made white-slipped serving ware from multiple recipes, while red- and black-slipped serving wares were made from one paste recipe each. These similarities and differences among the pastes of Middle Preclassic-period slipped serving wares suggest we may find both consistent and variable recipes for the slip on these ceramic groups as well.

Thesis Organization

The remaining chapters of this thesis will contextualize the research at hand in light of the use of pXRF spectrometry on ceramics and previous chemical analyses of ceramic surface finishes, discuss the chosen type: varieties and pXRF analysis conditions, present the chemical composition determined by pXRF analysis for slip of each type: variety, and evaluate what these results tell us about Middle and Late Preclassic slip recipes and the effectiveness of pXRF spectrometry for the chemical analysis of slip and other surface finishes.

Chapter 2, divided into two sections, provides background on pXRF spectrometry and previous chemical analyses of ceramic surface finishes. The first section begins with a brief

discussion of the science behind pXRF spectrometry, as well as its capabilities, advantages, and disadvantages, particularly as they apply to ceramics in general and slips in particular. The second section reviews chemical analyses that have been conducted on ceramic slips, glazes, and paints.

Chapter 3 discusses the materials and methods used in the research for this thesis. It begins with an overview of the Middle and Late Preclassic-period slipped serving ware traditions – Flores Waxy Ware and Paso Caballo Ware – and the characteristics of type: varieties that comprise them, focusing on those of interest in this thesis research: Joventud Red, Pital Cream, Chunhinta Black, Sierra Red, Flor Cream, and Polvero Black. The chapter then discusses the sample selection criteria used to obtain a 10% sample of the sherds of the six type: varieties excavated during the 2017 season of the Holtun archaeological project. The chapter ends with discussions of sample and data analyses. The former describes the sample preparation process and the conditions and procedures for pXRF analysis of trace elements in each sherd in the sample. The latter covers the statistical analysis procedures.

Chapter 4 presents the results and analysis of the region of interest (ROI) data and the calibrated data. The analysis of the semi-quantitative ROI and the calibrated data includes comparisons between the slipped surfaces on the sherd and a clean break to determine the extent to which the underlying paste is sampled in addition to the slip. The ROI data was evaluated by ranking the elements of interest from greatest to least based on relative abundance. The calibrated data first was evaluated through two-step cluster analyses to determine compositional groups. Chi-square analyses were then used to assess the relationship between obtained compositional groups and slip color type: variety, and architectural group.

Chapter 5 concludes the thesis with a review of the results, concentrating on the ability of pXRF spectrometry to characterize the chemical compositions of ceramic slips and the compositional groups obtained with the calibrated concentration data. The results of the statistical analysis for this data indicated that pXRF spectrometry can be successfully implemented in the chemical characterization of ceramic slips. Furthermore, the analysis revealed two distinct compositional groups based on the slip color. This chapter also explores the implications of the results for future chemical characterization studies of ceramic slips, addressing continued use to pXRF spectrometry on ceramic slips, further research on the sample, and chemical characterization studies of Middle and Late Preclassic-period slips overall.

CHAPTER 2: LITERATURE REVIEW

Chemical characterization studies require an understanding of both the analysis technique to be employed and the material to be analyzed. Here I provide an overview of how pXRF spectrometry works and its advantages and disadvantages as an analysis technique, especially as it applies to the study of archaeological ceramics in general. The focus then narrows to ceramic slips. The characteristics of slip and the reasons for its application are more thoroughly explored, and previous research on the chemical compositions of slips is reviewed. Given the absence of studies characterizing the chemical composition of ceramic slips and limited prior application of pXRF spectrometry to ceramic surfaces, this section includes chemical analyses of ceramic glazes and paints as well as studies conducted with other chemical analysis techniques.

pXRF Spectrometry

XRF spectrometry is a bulk analysis technique that measures the elemental composition of materials such as stone, glass, metal, and ceramic. The designation of a bulk analysis technique stems from a several square millimeter spot size and x-ray penetration sometimes extending through multiple layers of the sample (Liritzis and Zachaias 2012). XRF spectrometry may be performed with larger, stationary units in laboratories or portable instruments. Over the years, advances in x-ray tubes and detectors have rendered portable instruments more or less equal to larger laboratory ones (Liritzis and Zachaias 2012). However, because pXRF instruments do not possess a sealed chamber for analysis, they cannot measure the concentrations of lighter elements as accurately as non-portable laboratory units (Speakman et al. 2011). This is due to the inability to form a "true" vacuum. Additionally, pXRF instruments may lack "the

higher-powered software necessary for the deconvolution of spectra and quantification of data that is available in most laboratory-based instruments" (Speakman et al. 2011:2).

pXRF instruments have several key components. A pXRF instrument is typically mounted on a tripod for stabilization, though it can be held by the analyst. Mounting the instrument on a tripod keeps it in a specific location, which is especially valuable for longer analysis times and for keeping the instrument in the same place to analyze the same spot during multiple runs.

The x-ray tubes in pXRF instruments include anode targets, often made of metals such as rhodium, rhenium, silver, and tungsten (McGlinchley 2012; Shackley 2012b; Liritzis and Zachaias 2012). The ideal anode target for the instrument varies depending on the material to be analyzed.

Filters can be placed "between the x-ray tube and samples to modify the shape of the source spectrum," in effect optimizing analysis conditions for lighter or heavier elements (Shackley 2012b:27; see also McGlinchley 2012). The choice of whether to use a filter and which filter to use depends on the elements the researcher expects to find in the sample or is interested in measuring. Since a calibration can only be applied if the settings under which the calibration data and the sample data were collected are the same, the calibration also plays a role in selecting the filter to be used. The calibration similarly determines the chosen energy settings – kiloelectron volts (keV) and microamperes (μA) – and duration of analysis. The researcher may need to run multiple analyses with different filters and energy settings to collect the best data for all possible elements.

X-rays, Spectra, and Background Radiation

As the name suggests, XRF spectrometry relies on x-rays for analysis. X-rays are a high-frequency, high-energy form of electromagnetic radiation that are higher energy and frequency than ultraviolet radiation, but lower energy and frequency than gamma rays (Shackley 2012b). The relationship between x-rays and the other forms of electromagnetic radiation is shown in Figure 1.

XRF spectrometry uses a "polychromatic beam produced from radio-isotopes, x-ray tubes, or synchrotrons of short-wavelength/high-energy photons" that is emitted from an aperture in the instrument (Liritzis and Zachaias 2012:110). When the x-rays strike the sample, electrons are ejected from the atoms of constituent elements. In each atom that loses an electron, an electron from an outer atomic shell will take the place of the lost one and release energy in the form of a fluorescent x-ray (Hall 1960; Schlotz and Uhlig 2006). This released energy is what is measured in pXRF spectrometry. The wavelengths of the released fluorescent x-rays vary by element, forming characteristic radiations that allow analytical software to identify the elements present in the sample and convert their concentrations into peaks on a spectrum like the one in Figure 2 (Hall 1960; Schlotz and Uhlig 2006; Shackley 2012b; Liritzis and Zachaias 2012).

On a produced spectrum, the energies of the fluorescing elements are recorded on the x-axis and the intensity on the y-axis. The energies, measured in kiloelectron volts (keV), are the known fluorescent wavelengths for each element. An element may have multiple keV values depending on its isotopes and the number of electron shells; these differing values are termed Kα1, Kα2, Kβ1, Lα1, Lα2, Lβ1, Lβ2, and Lγ1, corresponding to naming conventions for electron shells.

	Gamma rays		X-rays		Ultraviolet	Visible Light		Infrared
Energy (keV)	1.24×10^{1}	1.24×10^{0}	1.24×10^{-1}	1.24×10^{-2}	1.24×10^{-3}	1.24×10^{-4}	1.24×10^{-5}	1.24×10^{-6}
Frequency (Hz)	10^{19}	10^{18}	10^{17}	10^{16}	10^{15}	10^{14}	10^{13}	10^{12}
Wavelength (m)	1×10^{-10}	1×10^{-9}	1×10^{-8}	1×10^{-7}	1×10^{-6}	1×10^{-5}	1×10^{-4}	1×10^{-3}

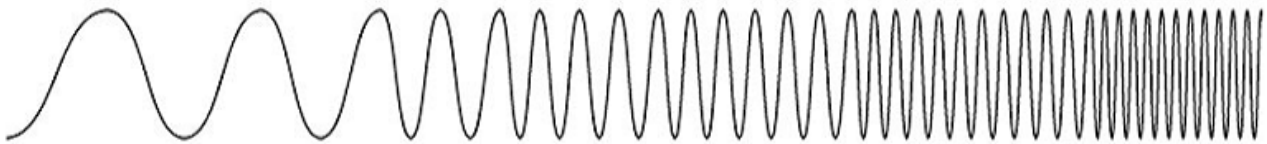

Figure 1. Energies, frequencies and wavelengths for the higher-energy forms of electromagnetic radiation. Figure by Anna Kebler.

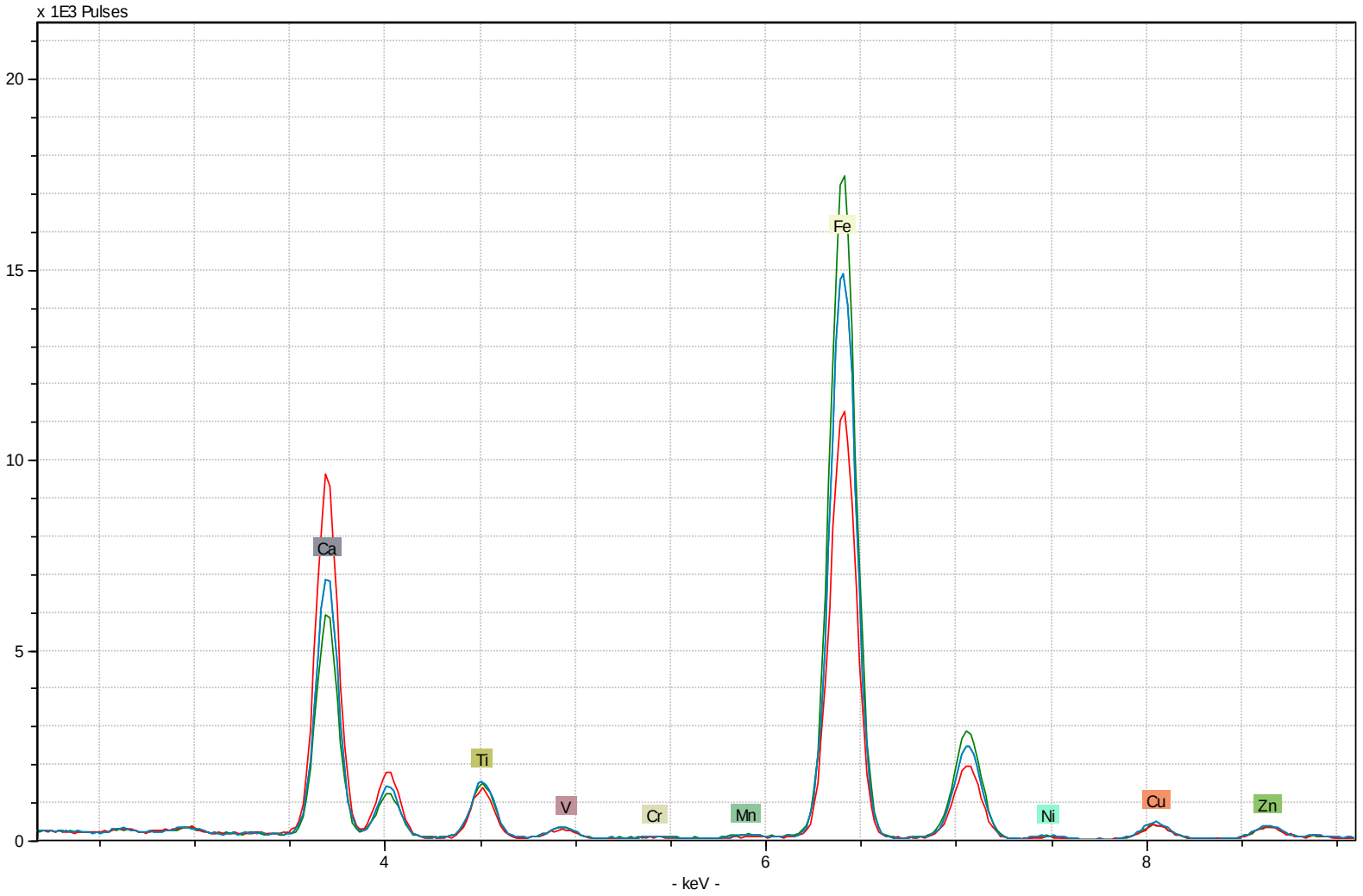

Figure 2. Compared spectra with elemental peaks labeled at characteristic emission energies. Figure by Anna Kebler.

Kα1 emission lines are most commonly used in XRF spectrometry, though other emission lines may be used if background radiation in the spectra, analysis conditions, and components of the instrument significantly affect the intensity of the Kα1 emission line (see Speakman et al. 2011 as an example).

Intensity is measured in photon counts per second (cps), providing a relative scale for assessing the concentration of each element in the sample (Hall 1960; Schlotz and Uhlig 2006; Liritzis and Zachaias 2012). This intensity measurement is an average, so using a 100-second live count will create a cps average of 100 data points. For qualitative results, the heights of the peaks appearing at the selected emission lines for elements can be compared. This allows the researcher to determine whether sample 1 has more, less, or about the same concentration of element X as sample 2. For quantitative results, weight percent and ppm concentrations for the Kα1 and other peaks of each element can be determined from this intensity data by applying an appropriate calibration to the produced spectrum.

The peaks in a spectrum, however, do not necessarily represent a one-to-one correlation with the concentrations of specific elements, and not every peak in a spectrum corresponds to the concentration of an element. There are multiple effects that impact the spectrum, creating additional peaks or seemingly amplifying the peaks already present. These effects include backscatter, bremsstrahlung radiation, Rayleigh scattering, escape peaks, Compton scattering, and sum peaks (Shugar and Mass 2012; Shackley 2012b).

Backscatter occurs as x-rays strike the sample and are scattered or reflected into the detector. Unlike other forms of background radiation, backscatter is stripped from analysis in instrumental XRF (Shackley 2012b). Bremsstrahlung radiation is what is often vernacularly referred to as background radiation. The “noise” that characterizes bremsstrahlung radiation

appears when electrons deaccelerate as they strike x-ray tube's anode. (Shackley 2012b; Schlotz and Uhlig 2006). The amount of bremsstrahlung radiation has an inverse relationship to the average atomic number of the elements that comprise a sample. For a sample made up primarily of light elements (i.e., those with lower atomic numbers), the amount of bremsstrahlung radiation will be greater than in a sample composed of heavier elements, i.e. those with higher atomic numbers (Shackley 2012b).

Unlike backscatter and bremsstrahlung radiation, Rayleigh scatter produces a source peak in the spectrum. This peak is the result x-rays striking the sample and being deflected without losing energy (Shugar and Mass 2012; Shackley 2012b). The peak that appears in the spectrum does not reflect the composition of the sample, but that of the anode in the instrument. Therefore, the analyst must know the type of anode their instrument contains to avoid including this peak as part of the sample.

Similarly, the composition of the detector creates additional peaks in the spectrum that are not a result of the composition of the sample. This occurs as x-rays strike the detector and diodes, causing the silicon that comprises them to fluoresce and creating escape peaks in the spectrum (Shackley 2012b). For any given element, an escape peak appears at the difference between the characteristic emission energy of that element and silicon (Schlotz and Uhlig 2006; Shackley 2012b). Iron (Fe), for example, has a Kα1 emission line at 6.40 keV, while silicon (Si) has a Kα1 emission line at 1.74 keV. The escape peak for iron thus occurs at ($keV_{Fe} - KeV_{Si}$), or 4.66 keV. While these peaks are always present, they are most apparent when a sample contains elements that strongly fluoresce (Shackley 2012b).

Sum peaks occur "when two characteristic fluorescent x-rays arrive at the detector at the same time, and so are experienced by the detector at twice the photon energy" (Shugar and Mass

2012:32). Continuing with iron as an example, its sum peak would occur at $2 \cdot keV_{Fe}$, or 12.8 keV. Some sum peaks may overlap and interfere with characteristic emission lines of other elements, as happens with the sum peaks of lead overlapping with the Kα peaks for cadmium and tin (Shugar and Mass 2012; McGlinchley 2012).

In cases where escape peaks and sum peaks interfere with characteristic emission peaks, the analyst must be able to recognize and filter out the escape and sum peaks by using different characteristic emission lines (such as the Lα lines) for the affected elements or by using calibrations or analysis software such as ARTAX that take into account the escape and sum peak photon energies for each element when identifying the elements reflected in a spectrum. Otherwise the results will not correctly characterize the elemental composition of the sample.

The last effect that alters the spectrum is Compton scattering. As with the other effects, it occurs as x-rays or released photons interact with the components of the XRF instrument. In the case of Compton scattering, it involves the target, which is often made of rhodium (Rh) in pXRF instruments used for archaeological analysis (Shackley 2012b). This results in the presence of large, broad Rh peaks in the spectrum. The Compton peak provides information about the mass of the sample, with a direct correlation between sample mass and the size of the Compton peak (Shugar and Mass 2012; Shackley 2012b). This relationship allows for better analysis of produced spectra in terms of both qualitative and quantitative data. Ratioing the characteristic emission peaks with the Compton peak allows for the comparison of samples of different masses, while calibrating known standards against the Compton peak quantifies the data through a process known as Compton normalization (Hall 1960; Shugar and Mass 2012; Shackley 2012b).

Elemental Detection Range

Once the background radiation is accounted for, an analyst can correctly identify the characteristic emission peaks and the elements to which they belong. Elemental range is restricted by the ability of the instrument's detector to accurately measure the fluorescent emissions of an element, and the conditions under which analysis is undertaken. According to Prudence Rice (1987), XRF spectrometry can produce data on around 80 elements. When optimizing conditions for the detection of each individual analysis, the often-advertised elemental range of XRF spectrometry extends from sodium (Na) to uranium (U) (Brouwer 2010).

The accuracy with which these elements can be measured varies, and not all these elements can be measured under the same conditions. The constraints on elemental range prevent pXRF units from analyzing sodium and elements with lower atomic numbers (Hall 1960; Shackley 2012b; Liritzis and Zachaias 2012). Elements with slightly higher atomic numbers, such as aluminum and silica, can only be measured under a vacuum (Hall 1960; Bezur and Casadio 2012; Speakman et al. 2011). Portable vacuum pumps are available, but as previously mentioned, pXRF units are unable to form a true vacuum because they lack an analysis chamber (Bezur and Casadio 2012; Speakman et al. 2011). Another means of improving detection for lighter elements in by flushing the unit with helium (Shackley 2012b; Hunt and Speakman 2015). On the other hand, XRF spectrometry is often well-suited to the analysis of elements with middling to high atomic numbers. According to Liritzis and Zachaias (2012:109), XRF spectrometry "is uniquely capable of detecting trace amounts of heavy elements, such as barium (Ba), antinomy (Sb), lead (Pb), and strontium (Sr)." Based on atomic mass and occurrence in inorganic archaeological material, the elements usually measured by XRF are potassium (K),

calcium (Ca), titanium (Ti), manganese (Mn), iron (Fe), zinc (Zn), arsenic (As) rubidium (Rb), strontium (Sr), zirconium (Zr), barium (Ba), mercury (Hg), and lead (Pb) (Liritzis and Zachaias 2012). The best results are produced for the nineteen-element range from titanium (Ti) and niobium (Nb) (Shackley 2012b).

The quality of data for elements greatly depends on the analysis conditions, including the atmosphere, filter and energy settings. Dry air can be replaced with a vacuum, or the instrument can be flushed with helium to produce higher-quality data for light-weight elements. Filters will absorb certain characteristic emission lines and more strongly excite elements with certain characteristic emission energies. For example, using a titanium filter, paired with a vacuum and energy settings of 15 keV and 55μA, allows x-rays with an energy between 3 to 12 keV to reach the sample (Speakman n.d.). This optimizes analysis for iron and lighter elements, excepting titanium and scandium.

Thus, while XRF spectrometry can analyze elements from sodium to uranium, high-quality data cannot be produced for all these elements at the same time. Conditions including atmosphere, energy settings, and filters must be changed to optimize detection for light, middling-weight, and heavy elements. This necessitates multiple runs under different analysis conditions to produce data for the full elemental range.

Applying XRF Analysis to Archaeological Ceramics

Archaeologists use XRF spectrometry to determine what elements within the established range are present in a sample, as well as its relative composition (Shackley 2012b). Elements detected by XRF and other chemical analysis techniques are usually categorized as major, minor, and trace based on their concentration. Major elements are present in concentrations of 2% or

more, minor elements in concentrations of 0.1% to 2%, and trace elements are present in concentrations of less than 0.1% (Barclay 2002; Rice 1987). Because trace elements are present in such small concentrations, they are often reported in parts per million (ppm).

The popularity of XRF spectrometry as an analysis technique stems from its practical advantages. It is non-destructive, fast, easy-to-use, requires minimal sample preparation, and can detect to the ppm level (Shackley 2012b; Liritzis and Zachaias 2012). XRF spectrometry's non-destructive nature remains a key draw for archaeological applications, as does the portability of pXRF instruments. These features allow for the analysis of objects that cannot be sampled or easily taken to a laboratory for other chemical analyses.

Yet XRF spectrometry is not ideal for the analysis of all archaeological materials. Characteristic elements must be within the established range. The bulk nature of the technique places limits on sample size, both in terms of spot size and depth. Finally, XRF spectrometry requires a certain degree of homogeneity in sample composition. All these limitations have implications for the analysis of archaeological ceramics.

Elemental Composition of Ceramics

When conducting chemical characterization studies of archaeological ceramics, we can expect major elements to include silica, aluminum, and oxygen. This is because most clays are "hydrous aluminum silicates," or are made up principally of silica ($2SiO_2$), aluminum oxide (Al_2O_3), and water (H_2O), though "the relative percentages of these three components…vary considerably in different kinds of clays" (Rice 1987:40). Iron, potassium, and calcium may be major or minor elements. Iron oxide – deriving from minerals such as hematite, goethite, limonite, magnetite, pyrite, marcasite, and siderite, or the silicates comprising a major portion of

the clay – are is the primary colorant for ceramic pastes and slips (Shephard 1956). Other minor elements in archaeological ceramics include sodium, magnesium, titanium, chromium, manganese, and nickel, while trace elements can include lithium, scandium, vanadium, cobalt, selenium, rubidium, strontium, antimony, cesium, tantalum, gold, uranium, and rare earth elements (Rice 1987). An additional element of interest one may expect to find on dark grey or black ceramic surfaces is carbon. This comes from deposits of carbon produced as byproducts of combustion during firing (Shephard 1956).

Many of the elements that characterize archaeological ceramics can be measured by pXRF technology. However, there are important elements that pXRF spectrometry cannot measure in certain conditions or at all. Important elements in ceramics, including oxygen, carbon, and sodium are not heavy enough to be measured by XRF spectrometry. Though much of the organic material used in forming ceramics burns out during the firing process, remnants of carbon – including smudging on the surface – will not be detected by XRF spectrometry.

One critical limitation of XRF is its inability to determine the compounds present in a sample, only the elements. To use the examples provided by Shugar and Mass (2012:26), XRF cannot distinguish between red lead(II, IV) oxide and litharge lead(II) oxide, nor copper carbonate and copper acetate. This may present a problem in determining the iron compounds that are prominent in many ceramics. However, XRF spectrometry can identify the trace elements that combine with iron to create the different minerals that may deposit iron in the clay used to make ceramics. This allows for some degree of chemical distinction between different clays. Furthermore, XRF spectrometry can be applied to raw clay and other soils as Neff, Voorhies, and Paredes Umaña (2012) have done, allowing for spectra of finished products and possible clay sources to be compared.

Spot Size, Penetration Depth, and Sample Homogeneity

The area analyzed on any given sample is a product of the size of the x-ray beam striking it. The beam diameter, in turn, is determined by the size of the aperture through which the beam passes. XRF units generally produce a beam diameter of approximately 4-10mm, resulting a spot size of approximately 15-22mm^2, with variability within this range depending on the aperture size of the instrument (Speakman et al. 2011; Ferguson et al. 2015, Rice 1987; Liritzis and Zachaias 2012; McGlinchley 2012). This spot size prohibits the analysis of extremely precise, small points. Instead, the instrument will collect bulk data about the chemical composition of the entire 15 to 22mm^2 area. This area should be flat and smooth, as curvature and roughness further the distance between the sample and the XRF instrument (Liritzis and Zachaias 2012).

The x-ray beam excites atoms located not just in the two-dimensional spot size area, but within its depth of penetration. How far an x-ray penetrates depends on the x-ray energy settings, the composition of the sample, the size of the sample, and the elements of interest (Bezur and Casadio 2012). Because of the variability in depth of penetration, Shackley (2012b) recommends that samples be at least 2mm thick. This figure is a catch-all estimate to account for a wide variety of energy settings and samples compositions. In terms of depth of penetration, all that is needed is for the sample to be infinitely thick for the irradiating x-ray to fully excite the atoms in the sample and for the detection of the wavelengths emitted by the excited atoms (Bezur and Casadio 2012). In other words, increasing the size or thickness of the sample will not lead to an increase in the intensity of a given wavelength emitted as a result of the x-ray excitation (Willis and Duncan 2008).

The size of the analysis area, the flatness of the sample, and the depth of penetration are of particular concern in the analysis of archaeological ceramics given their inherent

heterogeneity and frequent curvature. These features have led some analysts to eschew XRF spectrometry as an appropriate analysis technique for assessing the chemical characterization of ceramics.

Shugar and Mass (2012:28) state that a sample for XRF analysis should "be of homogenous material…and of uniform particle size." These qualities rarely describe archaeological ceramics. First, a ceramic is a layered structure, making it heterogeneous by definition. For a glazed or slipped ceramic, the layers include the surface finish, the body, an interaction zone between the two, any tempering materials, and the "intermingled vitreous and crystalline regions within the body" (Shugar and Mass 2012:28). Issues with homogeneity extend beyond the conscious decisions of potters in clay preparation and vessel formation and decoration, as they can be a product of firing processes or the clays themselves. According to Liritzis and Zachais (2012:119),

> clay's inhomogeneity, caused either by the presence of non-normally distributed inclusions or simply incomplete refinement processes, results in distribution issues. In pottery studies, it is also the high- or over-firing that can occur on a sub-set of artifacts produced at the same kiln that is responsible for alteration effects in the rare earth element concentrations.

Shackley (2012a) expands on the concerns about firing, stating that the heterogeneity of ceramics is a result of being fired at relatively low temperatures – especially for prehistoric potters working without kilns – compared to the over 1,000ºC-conditions at which volcanic rocks are naturally produced in Earth's mantle and crust.

Given the heterogeneity stemming from clay composition, multiple chemically distinct layers, and firing temperatures and atmosphere, we must consider how the makeup and shape of archaeological ceramics further affect studying them through XRF spectrometry. In addition, we

must consider how researchers can select and prepare ceramic samples that are best suited to the analysis technique.

The several-square-millimeter spot size of XRF spectrometry is advantageous when studying ceramics, since the relatively large area helps to mitigate the issues of heterogeneity and variable grain size on the surface or uppermost layers of a ceramic. Grains of various sizes, as well as aplastic inclusions such as temper, can be measured simultaneously to assess an average composition of the analysis area. In addition, obvious inclusions or discolorations can be avoided in spot selection. Heterogeneity on a ceramic surface primarily becomes significant in μXRF spectrometry. With a beam size of approximately 30-100 μm in diameter, the effects of heterogeneity become pronounced, as various ceramic grains or aplastic inclusions may be measured individually rather than collectively (Speakman et al. 2011). While the small spot size of a μXRF spectrometer may be valuable in assessing particularly small decorative elements, Ferguson et al. (2015) state the several-square-millimeter spot size of XRF spectrometers is enough to isolate many individual design elements when analyzing painted decoration on ceramics. Thus, the spot size involved in XRF spectrometry does not bar analysis of archaeological ceramics.

Since ceramic sherds frequently possess a curve as a result of the vessel form, ceramic samples will rarely be completely flat, particularly if they are large. This affects how close the sample can be placed to the instrument's aperture. The convex surface (usually the exterior) can be placed closer to the aperture than the concave surface (usually the interior). However, when Ferguson et al. (2015:323) compared the XRF data collected from interior and exterior surfaces of vessels, they found no changes unrelated to different chemical compositions, "indicating minimal, if any, impact as a result of variation in sample geometry." Surface roughness may

have a similarly minimal effect, though this is more easily controlled for through sample preparation or spot selection.

Depth of penetration can be determined through the chemical composition and density of the sample. Because silica is typically the most abundant constituent in ceramics, Drake (2018) has used it to calculate the depth of penetration for the analysis of certain common elements in ceramics. His values are listed in Table 1.

Table 1. Drake's (2018) depth of penetration values for selected elements of increasing mass.

	Emission Line	Energy (keV)	Depth of Penetration (mm)
Al	Kα1	1.47	0.02
Si	Kα1	1.74	0.03
P	Kα1	2.01	0.01
Ca	Kα1	3.69	0.06
Cr	Kα1	5.41	0.19
Fe	Kα1	6.40	0.30
Cu	Kα1	8.05	0.58
Zn	Kα1	8.63	0.77
Pb	Lα1	10.55	1.13
Zr	Kα1	15.78	3.84

These depth of penetration values reflect a trend. Elements that fluoresce at low characteristic energies have a lower depth of penetration, while those that fluoresce at higher energies have a higher depth of penetration. Thus, for light, low-fluorescence-energy elements like calcium, only amounts present in the surface layer will be measured. Heavier, high-fluorescence-energy elements like zirconium will be measured through the uppermost layers of the ceramic.

Furthermore, the atoms of each element excited will become increasingly restricted to the surface layer of the ceramic as the sample density increases. Drake's depth of penetration values

are based on silica's density of 2.648 g/cm^3. The actual densities will vary based on the ratios of aluminum oxide, silica, and water in a clay that comprises a ceramic, as well any additional major, minor, and trace elements found in the clay and any inclusions. As the sample becomes denser, the depth of penetration becomes shorter (Drake 2018).

Taking into account the relationships between depth of penetration, characteristic energies at which elements fluoresce, and sample density, it becomes apparent why the heterogeneous layered structure of ceramics is problematic for XRF spectrometry. Ceramics are largely more than a few millimeters thick, meaning not all potentially chemically-distinct layers will be analyzed. This leads to an only partial chemical characterization. For example, aluminum, one of the major constituents in clay, can only be measured up to 0.02mm below the surface. If there is any difference in the aluminum content of the small volume of ceramic analyzed versus the rest of the object, the chemical characterization will not accurately represent the ceramic as a whole.

Analysts have two main options to make up for the heterogeneity of archaeological ceramics. First, they can scrape away any paint, glaze, or slip and grind the isolated paste into a powder to increase the homogeneity of the sample (Liritzis and Zachaias 2012, Speakman et al. 2011). This is an imperfect solution. Grain sizes can still vary in powder, though how much this affects analysis depends on how chemically distinct samples are from one another (Liritzis and Zachaias 2012). Furthermore, it negates one of the major advantages of XRF spectrometry: its nondestructive nature. While the powder is not destroyed in the analysis, a piece of ceramic must be removed and altered in ways that can prevent further analysis. The limitations of x-ray beam size and depth of penetration and the demands they impose on sample size, shape, and

homogeneity frequently make XRF spectrometry a less-than-ideal analysis technique for ceramic pastes.

The second option analysts have in order to make up for the heterogeneity of archaeological ceramics involves bypassing the ceramic paste altogether. Analysts can adjust their research area to focus exclusively on surface treatments, including paints, glazes, and – most importantly for this thesis – slips. They are chemically distinct from the rest of the ceramic body, and, as the topmost layer of the ceramics, do not require significant depth of penetration for full chemical characterization. Additionally, they are often significantly smoother than the ceramic paste, negating any issues arising from sample roughness. These qualities make such surface treatments potentially ideal targets for chemical analysis via XRF spectrometry.

Ceramic Slips

Slips are defined by Rice (1987:149) as a fluid suspension of clay in water. Mixing clay particles into water allows for components to be more evenly distributed throughout the liquid, rather than potentially isolated in sections as a result of mixing and kneading solid clay and other components by hand. Slip usually lacks the aplastic inclusions used as temper in the ceramic paste, further decreasing the heterogeneity of ceramic slips.

Perhaps most critically, slips are a surface treatment. As stated by Cecil and Neff (2006), it is incredibly difficult to remove slip for analysis without extracting portions of the paste as well. Therefore, ideal techniques to chemical characterize slips can be used without removing small, pure portions for analysis. The non-destructive nature of XRF makes it ideal for such analyses, particularly since slips are often highly polished, resulting in a smooth surface for analysis (Shephard 1956). Furthermore, x-rays only need to penetrate the first layer (i.e., the

slip), no deeper. This reduces the issue of heterogeneous layers that many scholars cite as a principal reason not use XRF spectrometry on archaeological ceramics.

In addition to a lack of research on ceramics using XRF spectrometry, there is a lack of research into the chemical composition of ceramic slips. However, they have much to tell us. This is seen through what we know about their production and use, as well as the limited chemical characterization studies that have been performed on slips and other applied surface finishes and decorations, namely glazes and paints.

Production and Use of Ceramic Slips

Potters may apply slip to a ceramic vessel for several purposes. The most obvious is changing the color of the exterior and/or interior surfaces. With a slip, the potter can create a surface that is clearer and brighter in color than is possible to achieve for the ceramic body, though the physical and chemical advantages of the ceramic paste are maintained (Shephard 1956; Rice 1987). Slips may also be polished and smoothed to create a fine, lustrous surface (Shephard 1956).

Potters may also have employed slips for further decorative and practical advantages. White or very light-colored slips can function as a smooth undercoat for painted decoration or translucent slipping (Rice 1987). In terms of texture, the compression and reshaping of the clay particles fills the pores in the surface of the ceramic, rendering it less permeable and able to be scraped without ripping out larger grains, pitting and cracking the ceramic as a result (Shephard 1956). Since archaeologists cannot fully determine the extent to which past potters understood how polished slips reduced vessel permeability, their main advantages remain altering the ceramics' appearance.

Yet a potter cannot choose a slip based purely on its aesthetic qualities. Some of its physical and chemical properties must be similar to the paste that makes up the body of the ceramic. Anna O. Shephard (1956:67-68) lists three requirements for slip to be used on a given paste: 1) it "should adhere well to the body, neither peeling or crazing," in order to maintain a similar coefficient of expansion between the slip and underlying body; 2) it "should harden within the same temperature range as the body" so that both that neither the slip and body remain soft after firing nor are overfired; and 3) it should have a consistency with "sufficient covering power to conceal the body," which is a function of the slip's mineralogical composition, particle size, ions, and dispersion.

Further complicating matters, the color and other physical properties of slips can change as a result of the firing process. This means that raw clay may not accurately reflect the color of the fired product due to the chemical changes that will occur at different temperatures and different firing atmospheres (Shepard 1956; Rice 1987). Carbonaceous materials may partially or fully burn out depending on the temperature at which the ceramic is fired and the amount of oxygen in the firing atmosphere, the same factors determining the extent to which the clay oxidizes.

Shepard (1956) and Rice (1987) describe the major chemical constituents and processes that lead to different colors in raw clays and ceramics. Grey and black raw clays contain high amounts of carbonaceous materials; orange-red, brown, and cream raw clays contain various amounts of iron; and white clays are free of carbonaceous material or iron (Rice 1987). Other impurities also be present in smaller amounts, further affecting the color of both the raw and fired clay. Carbonaceous material burning out of clay can reveal the underlying iron content in the clay, resulting in pronounced differences between the grey or black raw clay and the cream,

buff, orange, red, or brown fired ceramic produced from it. The shade and hue of the latter set of colors depends on the amount of iron in the raw clay, its distribution, and the firing atmosphere. Grey and black fired ceramics can be produced when carbonaceous material is not fully burned out, ceramics are fired in a reducing rather than an oxidizing atmosphere, or carbon and other productions of the combustion process are deposited on the ceramic during firing.

Additional color changes can take place between applying the slip and firing the ceramic. According to Shephard (1956), polishing's compaction of clay particles creates a denser and more lustrous surface that generally results in a clearer and darker surface color. Further surface treatments, such as double slips, paints, and incised decorations can change the color of part or all of the ceramic surface. Absorbed stains and deposition of carbon from cooking fires during use, as well as the effects of soil after deposition, continue to alter the color of the fired ceramic after the manufacturing process is complete (Shepard 1956; Rice 1987).

Meeting all three of Shepard's criteria while maintaining a pleasing color requires that potters have detailed knowledge of the clays they use for slips. Potters must further balance these concerns with what materials are available locally and the technological and stylistic demands of the community. Surface finishing and other forms of decoration are important parts of the style and the sourcing, production, and application of slips remain important components of the *chaine operatoire* involved in producing a slipped vessel (Dietler and Herbich 1989; Chilton 1998). Furthermore, surface finishing and decoration can persist across time and space and are one of the most obvious parts of finished ware for a potter to copy (Bill 2013). Chemical research, then, not only reveals much about the process of pottery making in an individual community, but about how styles spread and are recreated, especially during a time of increasing specialization in pottery manufacture, as seen during the Preclassic period.

Chemical Characterizations of Slip, Glaze, and Paint

Currently, the defining chemical characterization studies of ceramic slips have been performed by Hector Neff and Leslie G. Cecil (Neff 2003; Cecil and Neff 2006; Cecil 2013). The studies use laser ablation-inductively coupled plasma-mass spectrometry (LA-ICP-MS) to study Postclassic-period Maya slips. In his 2003 study on the surfaces of plumbate pottery (pottery with a semi-vitrified slip), Neff was able identify slip composition and procurement areas that supported the idea that the clay for the plumbate slips, like that for the pastes, were sourced from multiple locations and produced locally in two distinct zones.

In 2006, Neff furthered his findings by studying more slipped and painted wares with Leslie G. Cecil. They were able to identify distinct compositional groups and used these to expand on what slip can tell us not only about ceramic production and specialization, but group identity. They write that "the Itzá and Kowoj (two antagonistic socio-political groups who lived in close proximity) used different pigments for exterior slips and paints used for decoration…[and] not only decorated their pottery with different motifs, but…the pigments that they used were decorative program-specific" (Neff and Cecil 2006:1490). Cecil (2013:200) later expanded on this pattern to slips, stating that "potters also appear to have been using different slips for different decorative programs." These variations in the chemical composition of slips and paints in addition to employed designs reveal deeply-entrenched and differentiated identities and indicate that the chemical characterization of slips is worthwhile.

Yet chemical characterization studies on ceramic slips have been limited. The pool of available studies becomes even smaller when limiting studies on slips to specific analysis techniques, such as XRF. With the lack of XRF spectrometry being applied to analyze ceramic

slips, we must consider how XRF has been applied to other surface finishes and decorations, particularly glazes and paints.

Bezur and Casadio (2012) studied glazes of porcelain wares using pXRF spectrometry. They analyzed "relatively thick (about 150-200 μm)" sections of clear and white glazes to assess the bulk composition of the glazes with regard to light elements such as aluminum, potassium, calcium, titanium, and iron. Because of the low depth of penetration for characteristic emission energies of these elements in silicates, data was collected purely from the upper glaze layer and was at least semi-quantitative. al-Saad (2002) has done similar research with glazed Islamic ceramics. By averaging the results from at least five randomly selected spots on each glazed surface, he was able to distinguish three distinct groups of glazes and their chemical constituents.

Ferguson et al. (2015) compared XRF data to LA-ICP-MS data for Southwestern ceramics and found that XRF spectrometry could identify sherds as belonging to the compositional groups previously defined by LA-ICP-MS analysis. The ability to identify the compositional groups previously defined by another technique was also observed by Speakman et al. (2011) when comparing the XRF analysis of ceramic pastes from Southwestern ceramics to previous research done with instrumental neutron activation analysis (INAA). Both argue that XRF is the weaker analysis technique, but has its advantages, especially when used for non-destructive surface analysis. Though Ferguson et al. (2015:362) state that LA-ICP-MS "is by far the superior approach to defining ancient paint recipes, it cannot be feasibly be applied to the analysis of whole vessels." The uniquely non-destructive abilities of pXRF spectrometry allow analysists to observe the compositional differences within vessels as well as between them, and to expand their sample size with *in situ* analyses while creating data for paints that can be compared with that from other analyses. The same needs to be done with ceramic slips.

Chapter Summary

XRF spectrometry determines the bulk elemental composition of a sample. Detectable elements range from aluminum to uranium, though different analysis conditions optimize data collection for certain elements. This often necessitates multiple runs with different analysis conditions to collect a full suite of elemental data for a sample. XRF spectrometry relies on x-rays produced by the instrument exciting a sample's constituent atoms, causing the emission of characteristic fluorescent energies that act as signatures for each element. The characteristic emission energies are plotted against their intensities to create a spectrum that can be used to determine the relative elemental composition for the sample. The spectrum, however, is not a pure reflection of the sample's elemental composition, as several background effects must be accounted for.

Even when the analyst adjusts for background radiation, there are potential complications when applying XRF spectrometry to archaeological ceramics. The most important concerns are the inherent heterogeneity of ceramics due to their mixed composition, layered structure, and irregularity in shape. The first two factors are particularly important because of the limited depth of penetration of the x-ray beam. Issues with the depth of penetration can be bypassed by grinding up the sample, though this negates XRF spectrometry's principal advantage of being nondestructive.

As an alternative, analysts can restrict analysis to smooth, more heterogeneous surface layers such as glazes, slips, and paints. This maintains the nondestructive nature of XRF spectrometry and allows for the analysis of components that cannot be studied when grinding samples. The impossibility of cleanly removing surface finishes and decorations for such preparation also prevents their analysis with XRF spectrometry.

The difficulty of removal seems to have resulted in little research the chemical compositions of surface finishes, particularly slips, or fluid suspensions of clays in water that are applied to the surface of a ceramic to change the surface color and texture. Nevertheless, the production and application of slips is an important part of the vessel creation process and one that can tell us much about ceramic production and specialization. This is apparent in the work done by Neff and Cecil (2006) on Late Preclassic-period Maya slips, which highlights the role ceramics play in sociopolitical identity. While this work was conducted using LA-ICP-MS, studies on glazes and paints applied to ceramic surfaces show that XRF spectrometry can determine the same compositional groups as LA-ICP-MS and INAA, with the advantages of non-destructiveness and in situ analysis allowing for the study of whole vessels and the increasing the sample size in studies using sherds.

CHAPTER 3: MATERIALS AND METHODS

This chapter provides an overview of the materials selected for the thesis and the methods used to analyze them. While the ancient Maya produced a wide variety of slipped type: varieties, this thesis focuses on red, cream, and black Middle and Late Preclassic-period type: varieties found at Holtun. The "Materials" section first describes the Middle and Late Preclassic-period slipped serving ware traditions, as well as the type: varieties of interest that comprise them. The research area, Holtun, is then discussed. Finally, the sample selection process and the sample itself are described. The "Methods" section consists of three parts: sample presentation, sample analysis, and data analysis. The data analysis section covers the procedures used for both the ROI and calibrated data.

Materials

Preclassic-Period Slipped-Ceramic Typologies of Interest

In the Maya lowlands, the slipped serving ware tradition is a relative constant throughout time periods. Across the region, we see iterations of this tradition in the form of K'an Slipped Ware, Flores Waxy Ware, Paso Caballo Waxy Ware, and Petén Gloss Ware (Adams 1971; Callaghan and Nievens de Estrada 2016; Gifford 1976; Kosakowsky 1987; Sabloff 1975). Common slip colors within these wares include red, orange, brown, cream, and black. Some type: varieties within these wares include additional surface treatments, such as incised decorations.

This thesis focuses on the Middle and Late Preclassic-period slipped serving ware traditions – Flores Waxy Ware and Paso Caballo Waxy Ware, respectively – which were

manufactured during times of increasing technological development and specialization in ceramic production.

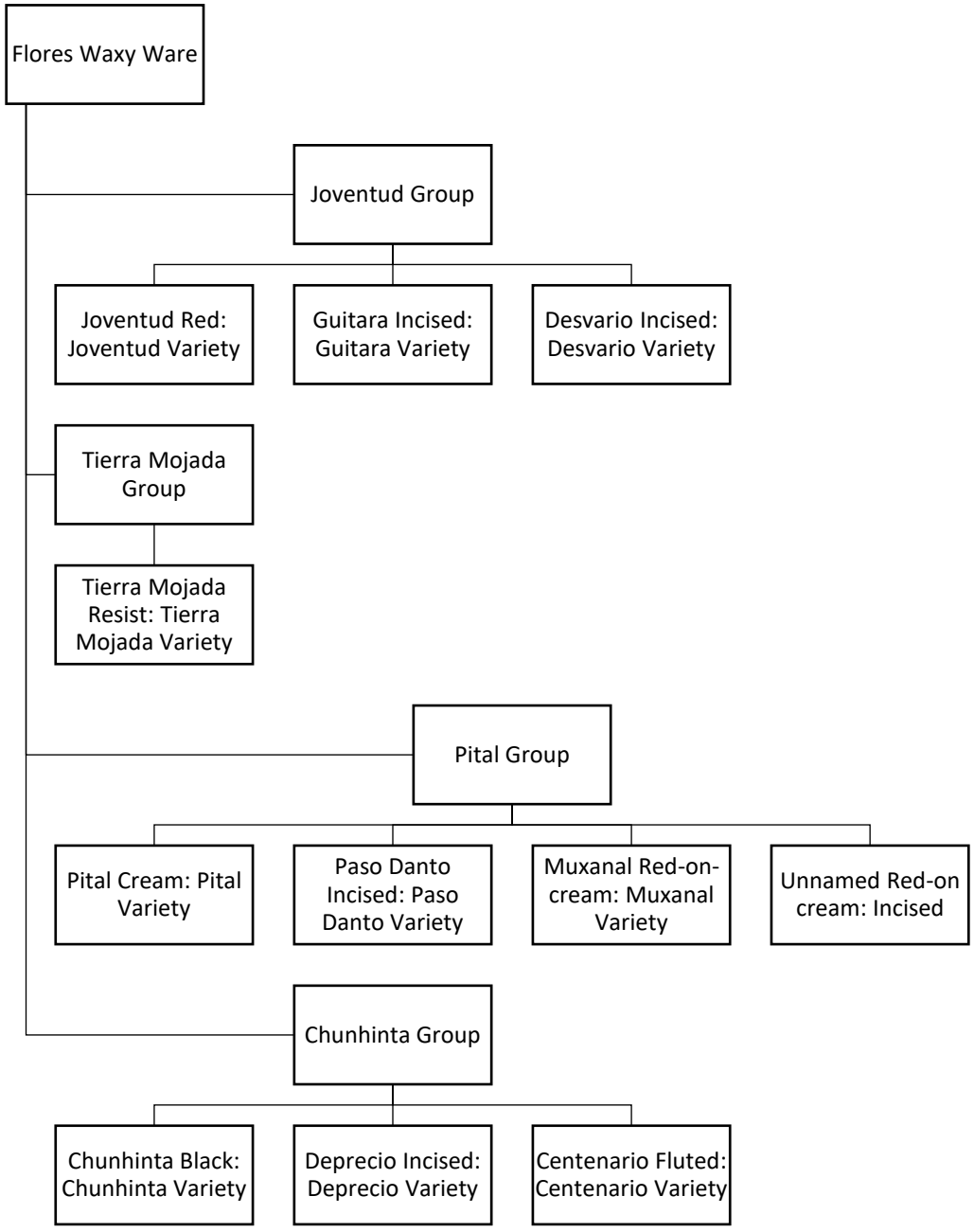

Figure 3. Type: varieties in the Middle Preclassic-period Flores Waxy Ware. Figure by Anna Kebler.

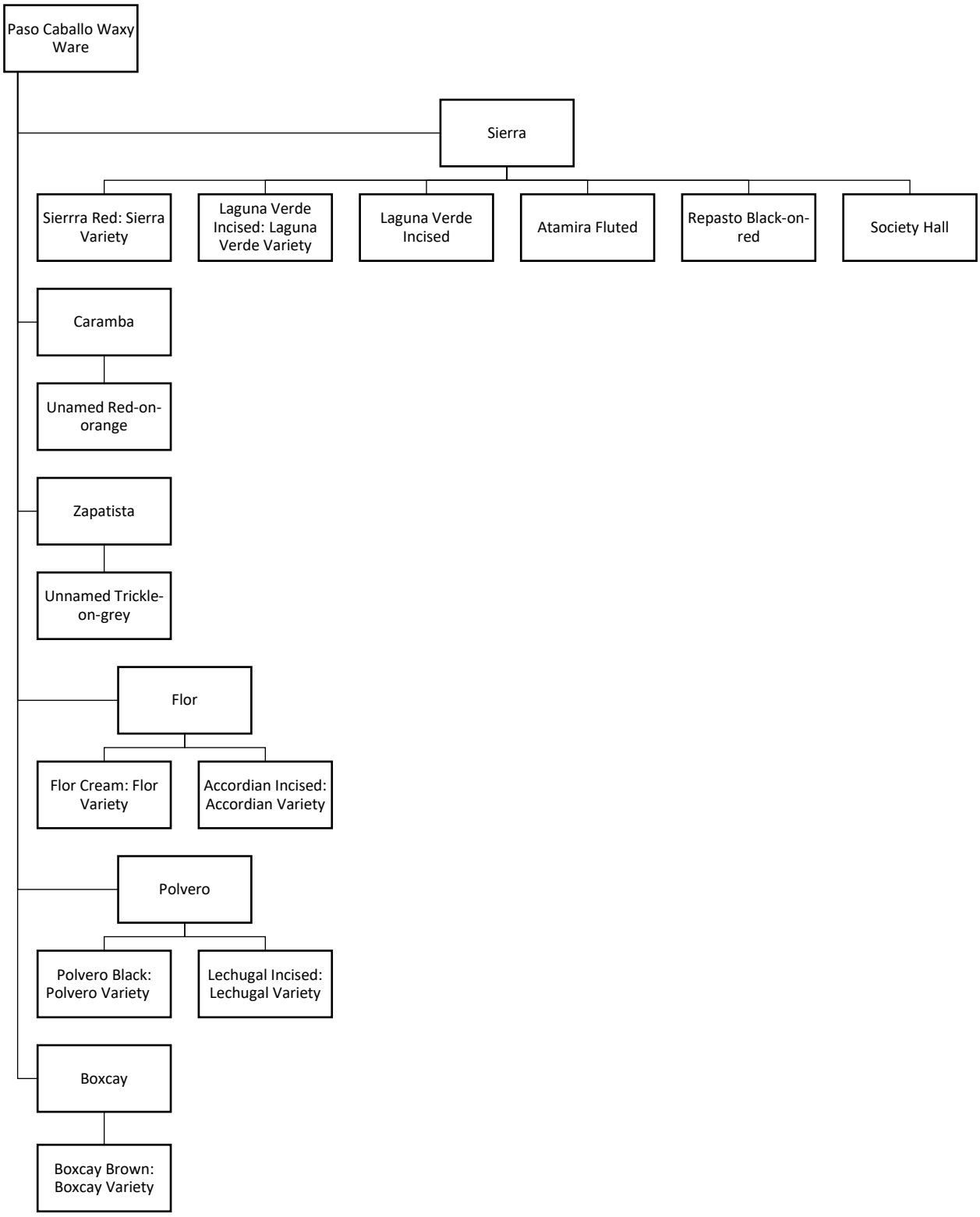

Figure 4. Selected type: varieties in the Late Preclassic-period Paso Caballo Waxy Ware. Figure by Anna Kebler.

Ceramics within the Flores Waxy Ware are characterized by "highly polished or burnished" slipped surfaces that "feel 'greasy' or 'waxy' to the touch" (Callaghan and Nievens de Estrada 2016:69). Figure 3 lists groups and type: varieties that make up Flores Waxy Ware. The Joventud and Tierra Mojada groups are red-slipped, tending more toward orange-red than the red slips seen during the Late Preclassic period; the Pital group is cream-slipped, tending more toward a true white than white slips seen during the Late Preclassic period; and the Chunhinta group is black-slipped (Callaghan and Nievens de Estrada 2016). The different type: varieties within each group are largely distinguished by the presence and type of surface decoration.

Ceramics within the Paso Caballo Waxy Ware share the "greasy" or "waxy" surface texture found in Flores Waxy Ware ceramics (Callaghan and Nievens de Estrada 2016:93). Figure 4 lists some of the groups and type: varieties within the Paso Caballo Waxy Ware. The Sierra group and the Caramba group are the red-slipped, tending more toward pure red than the orange-red slips seen during the Middle-Preclassic period; the Zapatista group has a cream wash with black trickle decoration; the Flor group is cream-slipped, tending more toward yellow than the cream slips seen during the Middle Preclassic-period; the Polvero group is black-slipped; and the Boxcay group is brown-slipped. Similarities in the color and texture of slips between corresponding Flores Waxy Ware and Paso Caballo Waxy Ware type: varieties, as well as similarities between the pastes and methods of manufacture, have led Forsyth (1989:13) to argue that the "Flores-Paso Caballo distinction makes no sense, since the Middle Preclassic and Late Preclassic-period ceramics that are essentially the same with respect to most factors." The extent to which these Middle Preclassic and Late Preclassic-period ceramic slips are chemically distinct is yet to be determined, though is one of the goals of this thesis.

Research Area

Holtun, located near the sites of Tikal and Yaxha, "is an intermediate sized civic-ceremonial center with documented occupation" from the Middle Preclassic-period to the Terminal Classic-period, from 600 BCE-900 CE (Callaghan et al. 2017:335). Built atop a karstic hill, the approximately 970 x 815m epicenter (Figure 5) "consists of 12 main groups and 80 structures all showing signs of stone construction" (Callaghan et al. 2017:335). Since many of the architectural groups have evidence of occupations in sealed, stratified deposits, there is ample material available for study and analysis.

The Holtun Archaeological Project began in 2010, focusing on the Middle and Late Preclassic-period occupations (Callaghan et al. 2017:335; see also Ponciano 1995; Fialko 2002; Kovacevich et al. 2011; Kovavecich et al. 2012a; Kovacevich et al. 2014; Cardona et al. 2015; Cardona et al. 2016; Cardona et al. 2017; Cardona et al. 2018). Its 2017 season maintained this focus, with excavations taking place in a range structure in Group F (HTN 2), the triadic pyramid in Group B (HTN 9), the plaza of Group C (HTN 11), the plaza of Group A (HTN 14), and households west of the monumental core of the site (various operations, including HTN 20, HTN 24, and HTN 25); these locations are marked in Figure 5. Excavations in each group uncovered sealed and stratified deposits containing Middle and/or Late Preclassic-period ceramics. This allowed for a representative sample of slipped ceramics from these periods at Holtun to be compiled.

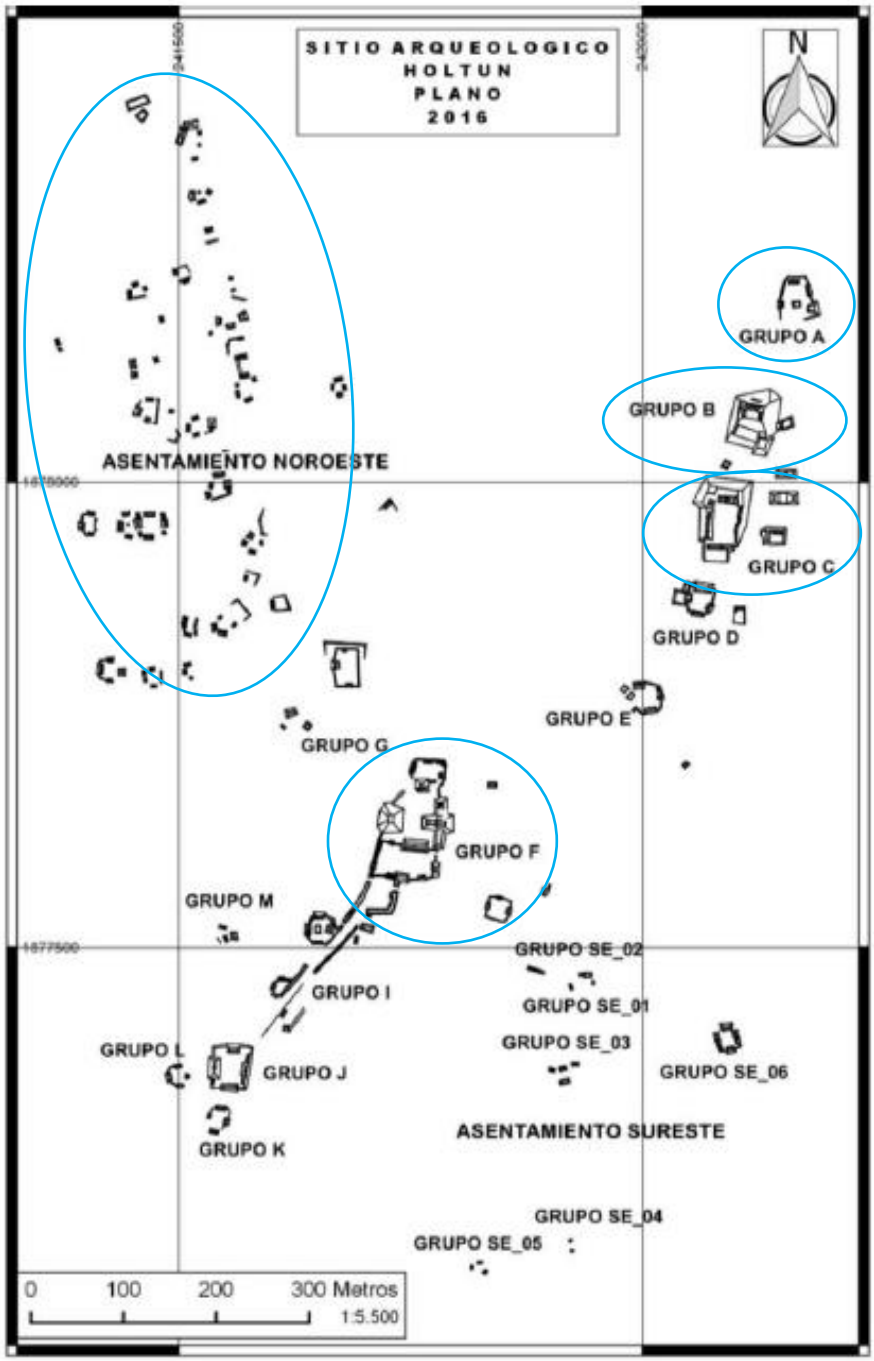

Figure 5. Site plan of Holtun, with relevant groups circled (Guzmán Piedrasanta 2016)

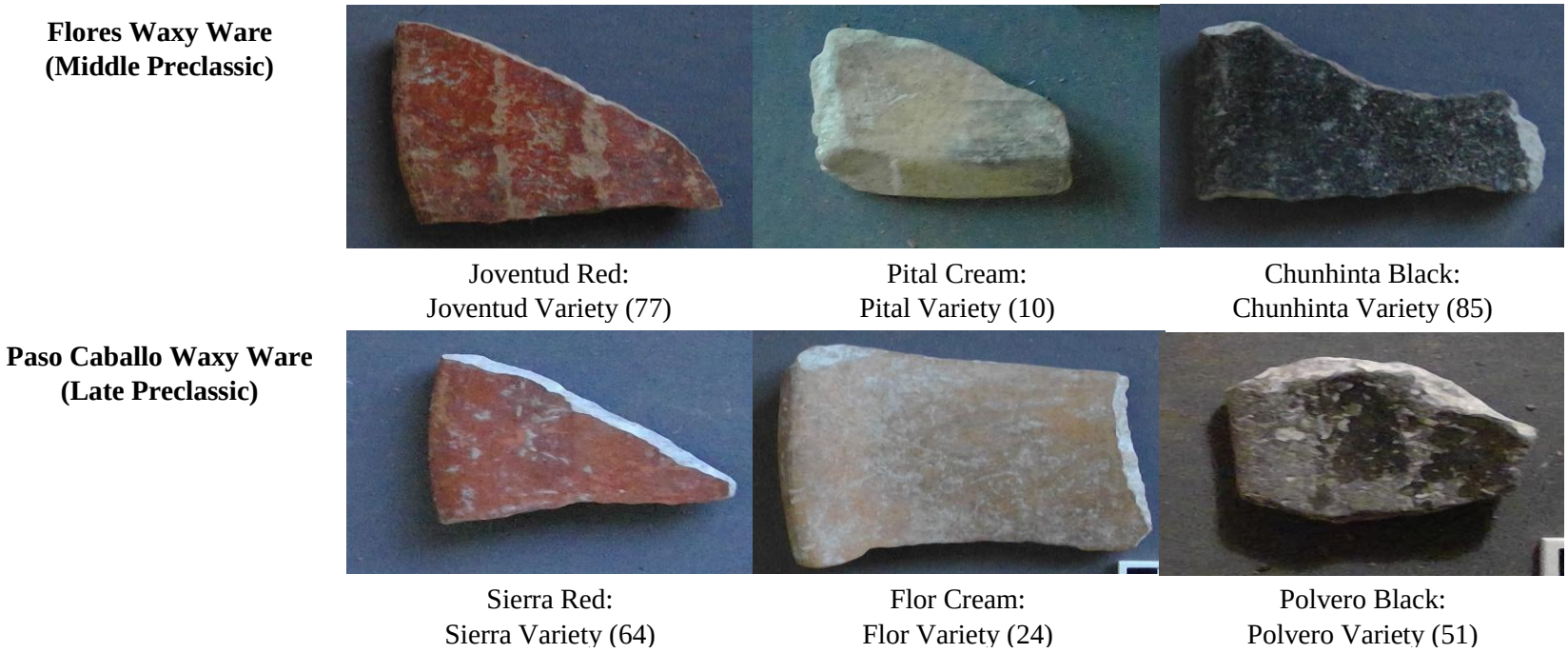

Figure 6. The type: varieties included in the sample, with the number of sherds included for each type: variety in parentheses. Photos by Anna Kebler.

Sample

The sample consists of 315 slipped sherds from Middle and Late Preclassic-period deposits excavated during the 2017 season of the Holtun Archaeological Project. Middle Preclassic-period sherds in the sample are Joventud Red: Joventud Variety (red slip with no other decoration), Chunhinta Black: Chunhinta Variety (black slip with no other decoration), and Pital Cream: Pital Variety (cream slip with no other decoration). Late Preclassic-period sherds in the sample are Sierra Red: Sierra Variety (red slip with no other decoration), Polvero Black: Polvero Variety (black slip with no other decoration), and Flor Cream: Flor Variety (cream slip with no other decoration). These type: varieties and number of each in the sample are shown in Figure 6. The three type: varieties for each period were chosen for analysis because they represent the otherwise-undecorated red, black, and cream slips for the Flores Waxy and Paso Caballo Waxy Wares. No slipped sherds with other forms of surface decoration (for example, incised sherds) were included in the sample to ensure a smooth surface was available for analysis.

After all the sherds of the six type: varieties excavated during the 2017 season of the Holtun Archaeological Project were tallied, a 10% sample of rim sherds for each type: variety was selected. 10% was selected as a representative (yet manageable) sample for all sherds of each type: variety of interest that were uncovered during the season. Rim sherds were used to limit the amount of times a single vessel was included in the sample, as there are a finite number of sherds that can come from a rim of a given diameter. The rim sherds can be used to calculate a minimum number of vessels (MNV), akin to the minimum number of individuals (MNI) in faunal analysis (Rice 1987:292). There were not enough rim sherds for 10% samples of all the 2017 Chunhinta Black: Chunhinta Variety and Polvero Black: Polvero Variety sherds. Therefore,

several well-preserved body sherds for these two type: varieties were included to achieve the desired 10% samples. When more rim sherds were available than necessary to generate a 10% sample, consisting entirely of rim sherds, of all 2017 sherds of the type: variety, sherds were first chosen to make sure all architectural groups where a given type: variety was found were represented. Sherds were then selected for the sample based on preservation, size, and random sampling. Where possible for every level of each excavation unit, sherds from different vessel types or from vessels of different rim diameters were selected to reduce sampling the same vessel multiple times. The breakdown of samples can be found in the Appendix.

Of the 315 sherds, only 311 were analyzed as four Sierra Red sherds (HTN17107, HTN17108, HTN17124, and HTN17125) and one Flor Cream sherd were not exported. Additionally, the exteriors of three Polvero Black sherds (HTN17300, HTN17302, and HTN17307) and the interiors of one Sierra Red sherd (HTN17081), one Pital Cream sherd (HTN17150), two Chunhinta Black sherds (HTN17187 and HTN17230), and one Polvero Black sherd (HTN17275) were not included in the tabulated analysis values because these surface were either unslipped or had degraded to such a degree that there was no analyzable slip on these surfaces.

Methods

Sample Preparation

Prior to exportation from Guatemala, a small section of each sherd was removed to produce a clean break so paste and slip could be observed in profile and analyzed without any discoloration or contamination. Sherds were photographed, rim diameters were measured, and rim profiles were drawn. Munsell color values were recorded for the slipped surfaces (exterior,

interior, or both) of all red- and cream-slipped sherds and for the pastes seen in the clean breaks of all sherds. These values are provided in the Appendix.

pXRF frequently requires “little or no pre-treatment” outside of gentle cleaning to remove surface contamination (Shackley 2012b:8-9). Each sample was cleaned with water after its excavation. The cleaned sherds were then sorted into their respective type: varieties by Dr. Michael Callaghan. In the lab, sample surfaces were cleaned again with distilled water and cotton swabs, with special attention being given to areas of well-preserved slip large enough for pXRF analysis.

Sample Analysis

All sherds were analyzed with a Bruker Tracer III-SD handheld XRF spectrometer equipped with a rhodium anode and a Silicon Drift Detector (SDD) with a resolution of 145 ev at the Mn $K_{\alpha 1}$ line (5.89 keV) at data acquisition rates of 100,000 counts per second. The unit’s spot size was 3mm x 4mm. Each sample was analyzed at 40 keV 11.30µA with a TiAl (yellow) filter placed in the x-ray path for a 200-second live-time count. These energy and time settings were selected to match those used in the Mudrock trace elements calibration, allowing it to later be applied to the collected data. The relatively long analysis time also allowed for a smoother, cleaner spectrum as a result of averaging the 200 data points for the concentrations of each element

Each sherd was analyzed three times. The clean break – a cross-section of the sherd comprising of both of the slipped surfaces, the paste, and any zones of interaction that is created after excavation and cleaning so that contamination from use and deposition is not a concern– was analyzed first. The ratio of slipped surfaces, paste, and interaction zones differs for each

sherd based on the thickness of slip and paste. This means that the elemental composition of the clean break would be similar if the analysis of the slipped surfaces extended through the slip and into the paste. Generating data for the clean breaks allowed for the depth of penetration to be tested, and therefore the appropriateness of pXRF spectrometry for the analysis of each element of interest to be determined.

The combination of analyzing clean breaks and comparing the data for clean beaks and slipped surfaces with statistical tests for comparing means was developed for this thesis in order to generate data on depth of penetration for each sherd while preserving as much of each sherd as possible for future analyses. This would not be possible with grinding up a portion of the sherd – including the paste, slip, and interaction zones – to determine its bulk composition for comparison with slipped surfaces. This technique did result in many clean breaks not being completely flush to the aperture, as well as small portions of the aperture being uncovered for some of the thinnest sherds. The effects of the partially-uncovered aperture merit further investigation as they may influence results, though Ferguson et al.'s 2015 work suggests that small quantities of dry air between the aperture and sample do not significantly affect the results.

After the clean break, both the exterior and interior slipped surfaces were analyzed. Each surface was only analyzed once because of the limitations imposed by the size of the analysis area, sample curvature, and slip preservation. The sample was positioned so that a section of well-preserved slip was placed as close as possible to the pXRF unit's aperture.

Elements of interest for the analyses of clean breaks and both the interior and exterior slipped surfaces were calcium (Ca), titanium (Ti), chromium (Cr), manganese (Mn), iron (Fe), cobalt (Co), nickel (Ni), copper (Cu), zinc (Zn), arsenic (As), rubidium (Rb), strontium (Sr), yttrium (Y), zirconium (Zr), niobium (Nb), molybdenum (Mo), rhodium (Rh), tin (Sn), antinomy

(Sb), barium (Ba), lead (Pb), uranium (U), and thorium (Th). Kα1 lines were used for all elements save barium, uranium, and thorium, for which the Lα1 lines were used. Analyses produced two types of data about the amounts of these elements in the sample: uncalibrated region of interest (ROI) data and calibrated ppm data. When conducting XRF analysis, ROI data is a type of semi-quantitative data produced by ratioing the counts for each elemental escape peak with the Compton peak, i.e. Compton normalization (McGlinchley 2012). ROI data reflects the relative abundances of each element of interest in the sample and thus the relative composition of the sample overall. It can provide a big-picture view of sample composition and is useful for comparing the compositions of multiple samples where calibrations are not present or less-than-ideal (Barclay 2002; Bruker n.d.).

The issue of appropriate calibrations is one of frequent concern for studies of archaeological ceramics. Bruker (2013) advocates the use of its Mudrock calibrations for these ceramics. However, such calibrations are principally designed to analyze modern materials and may be ill-equipped to analyze the heterogeneity of ceramics, particularly low-fired ones (Aimers et al. 2012; Shackley 2012b). As addressed in Chapter 2, however, slips are more homogenous than ceramic pastes, reducing concerns stemming from heterogeneity. This makes the Mudrock calibration less-than-ideal, but readily available to produce ppm concentration data from which an estimate of compositional groups can be derived.

Data Analysis

ROI Analysis

Mean relative abundances for each element of interest were calculated for both the slipped surfaces and the clean breaks. The means calculated from the ROI data were first used to

assess whether pXRF analysis was extending past the slip and into the paste when measuring relative abundances. This was evaluated by comparing the mean relative abundance for each element of interest in the slipped surfaces versus in the clean breaks. Since multiple distributions of relative abundances for each element were non-normal, the more conservative two-tailed Mann-Whitney U test was applied to compare the means. If, for any elements, the means for clean breaks and slipped were not significantly different at the 95% confidence interval, the elements in question were excluded from subsequent analyses with the ROI data.

Means for the remaining elements of interest in the slipped surfaces were calculated for each type: variety. Using these means, the remaining elements of interest were then ordered from most abundant to least abundant. Any differences in element orders between type: varieties were noted, as were noticeable differences in mean values. These differences indicated elements that would potentially distinguish between compositional groups in the calibrated data.

ppm Concentration Analysis

Mean relative abundances for each element of interest were calculated for both the slipped surfaces and the clean break. Whether pXRF analysis was extending past the slip and into the paste when measuring calibrated concentrations was assessed through the same procedure used for the ROI data. This was evaluated again to account for any changes in the magnitude of similarities and differences in mean values caused by applying the calibration. If, for any elements, the two-tailed Mann-Whitney U test indicated that the means for clean breaks and slipped surfaces were not significantly different at the 95% confidence interval, the elements in question were excluded from subsequent analyses with the ppm data.

The concentrations of the remaining elements of interest in the slipped surfaces were subjected to two-step cluster analyses, which generate distinct compositional groups (see Glascock 1992, among others). Cluster analyses were run until the cluster quality was fair-to-good in terms of the silhouette measure of cohesion and separation, with the elements least important to predicting cluster membership being removed from subsequent cluster analyses until the desired cluster quality was achieved.

After the final cluster analysis determined compositional groups with the desired cluster quality, chi-squared tests of association were run to assess the relationship between compositional group membership and slip color overall and type: variety specifically. The relationship between the compositional groups and architectural groups where sherds were excavated was assessed using chi-square goodness-of-fit tests, with compositional group membership by slip color and type: variety used to calculate expected proportions. The results of these chi-square tests allowed for the identification of any significant compositional differences between sherds of different type: varieties and colors, as well as those from different architectural groups.

Summary

The sample for analysis consisted of 315 sherds (313 rim sherds and 2 body sherds) belonging to the otherwise undecorated red-, cream-, and black-slipped type: varieties of the Middle and Late Preclassic-period slipped serving wares. For the Middle Preclassic-period Flores Waxy Ware, this included Joventud Red: Joventud Variety, Pital Cream: Pital Variety, and Chunhinta Black: Chunhinta Variety. For the Late Preclassic-period Paso Caballo Waxy Ware, this included Sierra Red: Sierra Variety, Flor Cream: Flor Variety, and Polvero Black:

Polvero Variety. 10% samples of each of the six type: varieties were created, with each architectural group where the given type: variety was excavated being represented.

A clean break, the exterior slipped surface, and the interior slipped surface of each sherd were analyzed using pXRF spectrometry. Calcium (Ca), titanium (Ti), chromium (Cr), manganese (Mn), iron (Fe), cobalt (Co), nickel (Ni), copper (Cu), zinc (Zn), arsenic (As), rubidium (Rb), strontium (Sr), yttrium (Y), zirconium (Zr), niobium (Nb), molybdenum (Mo), rhodium (Rh), tin (Sn), antinomy (Sb), barium (Ba), lead (Pb), uranium (U), and thorium (Th). Two types of data were produced: uncalibrated ROI data and concentrations in ppm generated with the Mudrock trace element calibration. For both types of data, whether the x-ray beam was extending through the slip and into the paste was evaluated to assess the ability of pXRF spectrometry to analyze the slipped surfaces alone. This was done by using the Mann-Whitney U test to compare the mean relative abundances or the concentrations, depending on the type of data, for each element in the slipped surfaces and the clean breaks. ROI data was then used rank the elements of interest based on relative abundance for each type: variety. For the ppm concentrations, two-step cluster analyses were run to distinguish compositional groups, and chi-squared tests of association were run to test the relationships between these groups, type: varieties, and overall slip color. To test the relationship between compositional group and architectural group, chi-square goodness-of-fit tests were run. These tests allowed for the determination of any significant variations in the chemical composition of slips by color, type: variety, and architectural group.

CHAPTER 4: ANALYSIS

This chapter provides the results of the data analysis. It begins with the semi-quantitative region of interest (ROI) data and continues on to the calibrated data. For both types of data, the first statistical procedures determined whether pXRF analysis was isolated to the surface. For the ROI data, relative abundances were ranked and differences in element order and quantity were noted. For the calibrated data, compositional groups were determined using two-step cluster analyses and chi-square analyses assessed the relationship between resultant compositional groups and slip color, type: variety, and architectural group.

ROI Data

Break vs. Slip

Using the ROI data, mean relative abundances for the elements in question in the slipped surfaces and clean breaks were calculated for each type: variety. The tabulated means are listed in Tables 2 and 3 below.

For each element measured, the null hypothesis was that there would be no difference between its mean relative abundance for the clean break and its relative abundance for the slip. For calcium, chromium, iron, cobalt, nickel, copper, arsenic, lead, thorium, rubidium, uranium, strontium, yttrium, niobium, molybdenum, rhodium, tin, and antimony, $p < 0.001$. For zinc, $p = 0.002$ and for manganese, $p = 0.009$. Therefore, we can reject the null hypothesis that there is no difference between the clean break and slipped surfaces' mean relative abundances of these elements at the 95% confidence interval. This suggests that pXRF spectrometry was successfully isolated to the slipped surfaces for calcium, chromium, manganese, iron, cobalt, nickel, copper,

zinc, arsenic, lead, thorium, rubidium, uranium, strontium, yttrium, niobium, molybdenum, rhodium, tin, and antimony when evaluating relative abundances.

Table 2. Mean relative abundances of the elements of interest in the slipped surfaces of sherds from each type: variety.

	Joventud Red	Sierra Red	Pital Cream	Flor Cream	Chunhinta Black	Polvero Black
CaKa1	2.549349	4.323635	3.134637	3.6817	3.974339	4.451233
BaLa1	1.405313	1.340726	1.891984	1.757767	1.905589	1.798695
TiKa1	1.657932	1.577846	2.217821	2.079007	2.251242	2.120672
CrKa1	0.288521	0.294302	0.265279	0.274657	0.281053	0.294487
MnKa1	0.440445	0.432243	0.442847	0.44845	0.396927	0.464308
FeKa1	46.80766	43.8929	36.85726	35.96822	37.04042	37.20049
CoKa1	3.359229	3.108458	2.792689	2.65935	2.686083	2.694526
NiKa1	0.329121	0.315334	0.311558	0.302546	0.30208	0.359563
CuKa1	0.657912	0.707106	0.775442	0.779274	0.797047	0.812276
ZnKa1	0.706914	0.742721	0.925853	0.811857	0.84749	0.789114
AsKa1	0.636682	0.65273	0.749753	0.754976	0.730378	0.747318
PbLa1	0.639285	0.655765	0.752216	0.758859	0.73374	0.750872
ThLa1	1.540105	1.624876	1.964616	2.00933	1.973343	1.99328
RbKa1	2.483352	2.585224	3.245116	3.308383	2.930024	2.786084
U La1	1.914119	2.023465	2.450595	2.534263	2.440195	2.429471
SrKa1	3.003877	3.067554	3.726621	3.6803	3.870083	3.605513
Y Ka1	2.857501	2.973348	3.686321	3.740363	3.452439	3.560113
ZrKa1	7.983226	7.450321	8.541284	8.513002	7.795056	7.393915
NbKa1	3.255092	3.401237	4.058726	4.124522	4.02561	4.013719
MoKa1	3.69087	3.873895	4.549863	4.681467	4.542965	4.55823
RhKa1	8.854559	9.614981	10.69747	10.96254	10.95819	11.06688
SnKa1	2.628671	2.838787	3.1741	3.284511	3.226552	3.251948
SbKa1	2.310264	2.502535	2.787942	2.884674	2.83904	2.857172

Table 3. Mean relative abundances of the elements of interest in the clean breaks of sherds from each type: variety.

	Joventud Red	Sierra Red	Pital Cream	Flor Cream	Chunhinta Black	Polvero Black
CaKa1	6.247068	8.666175	6.18091	5.284761	7.663059	9.068623
BaLa1	1.213675	77.5083	1.87307	1.901865	1.992398	1.987253
TiKa1	1.425655	90.8641	2.19884	2.24943	2.346354	2.344239
CrKa1	0.273631	17.6845	0.25713	0.26363	0.262417	0.272788
MnKa1	0.510269	34.2955	0.43105	0.487209	0.392984	0.470768
FeKa1	41.37061	2390.928	32.45352	31.65246	31.12487	28.68602
CoKa1	2.964203	171.1148	2.44329	2.348504	2.299579	2.133399
NiKa1	0.253213	16.4329	0.24594	0.252239	0.257156	0.286953
CuKa1	0.740412	50.3593	0.84099	0.918196	0.911677	0.975277
ZnKa1	0.720577	47.371	0.8419	0.878374	0.858356	0.869208
AsKa1	0.649387	43.5024	0.7716	0.799391	0.771773	0.818394
PbLa1	0.652153	43.7185	0.77508	0.804039	0.776681	0.822278
ThLa1	1.657931	112.0304	2.0807	2.199226	2.174315	2.274096
RbKa1	2.605482	173.5857	3.40996	3.4838	3.135247	3.109634
U La1	2.064499	139.2072	2.60714	2.75317	2.670518	2.757992
SrKa1	3.463213	220.7299	4.01216	4.088496	4.236375	4.030384
Y Ka1	3.070678	206.2302	3.87589	4.008791	3.737718	3.966483
ZrKa1	7.738071	476.1982	8.33528	8.292774	7.590178	7.563826
NbKa1	3.475217	233.1041	4.26111	4.379748	4.295272	4.41895
MoKa1	3.954786	266.0714	4.77015	4.954057	4.836117	4.978337
RhKa1	9.64977	666.6303	11.17899	11.53587	11.40686	11.79165
SnKa1	2.823279	195.5973	3.28533	3.437752	3.306211	3.40161
SbKa1	2.476175	172.2001	2.86993	3.026204	2.889342	2.97172

However, several sets of means were not significantly different. For barium, $p = 0.510$; for titanium, $p = 0.476$; and for zirconium, $p = 0.650$. Therefore, we accept the null hypothesis that there is no difference between the clean break and slipped surfaces' mean relative abundances of these elements at the 95% confidence interval. This suggests that pXRF spectrometry consistently extended past the slipped surface and into the paste when measuring relative abundances of barium, titanium, and zirconium. Because of this, these three elements will be excluded from the following ROI analysis. Calibrated ppm analyses also showed that the

only significant source of rhodium was the pXRF unit itself. Therefore, rhodium will also be excluded from the following analyses.

Comparing the Relative Abundance Means for Slipped Surfaces

Table 4 shows the relative abundances of each element ordered from greatest to least. Elements whose ranked relative abundances differ between type: variety are highlighted. For all type: varieties, iron was the most abundant element. The second- through tenth-most abundant elements differed by type: variety, as did the thirteenth- and fourteenth-most abundant. The most significant difference in rankings is for cobalt. For Joventud Red slips, it is the third-most abundant element. For Sierra Red, it is the fifth-most abundant. For Pital Cream, it is the ninth-most abundant. Finally, for Flor Cream, Chunhinta Black, and Polvero Black, it is the tenth-most abundant. When considering the percent relative abundance as well as the rankings, many of the difference are small. The largest difference in percent relative abundance is in iron, as Joventud Red and Sierra Red slips have noticeably higher relative iron content than Pital Cream, Flor Cream, Chunhinta Black, and Polvero Black slips. Collectively, these data indicate that calcium, iron, cobalt, zinc, rubidium, strontium, yttrium, niobium, molybdenum, tin, and antimony are primary elements of interest when determining compositional groups. Of these, iron and cobalt stand out as the most promising for distinguishing between groups based on the magnitude of difference in concentrations between type: varieties.

Table 4. Ranked mean relative abundances of elements of interest for the slipped surfaces of sherds of each type: variety.

	Joventud Red	Sierra Red	Pital Cream	Flor Cream	Chunhinta Black	Polvero Black
1st	FeKa1	FeKa1	FeKa1	FeKa1	FeKa1	FeKa1
2nd	MoKa1	CaKa1	MoKa1	MoKa1	MoKa1	MoKa1
3rd	CoKa1	MoKa1	NbKa1	NbKa1	NbKa1	CaKa1
4th	NbKa1	NbKa1	SrKa1	Y Ka1	CaKa1	NbKa1
5th	SrKa1	CoKa1	Y Ka1	CaKa1	SrKa1	SrKa1
6th	Y Ka1	SrKa1	RbKa1	SrKa1	Y Ka1	Y Ka1
7th	SnKa1	Y Ka1	SnKa1	RbKa1	SnKa1	SnKa1
8th	CaKa1	SnKa1	CaKa1	SnKa1	RbKa1	SbKa1
9th	RbKa1	RbKa1	CoKa1	SbKa1	SbKa1	RbKa1
10th	SbKa1	SbKa1	SbKa1	CoKa1	CoKa1	CoKa1
11th	U La1	U La1	U La1	U La1	U La1	U La1
12th	ThLa1	ThLa1	ThLa1	ThLa1	ThLa1	ThLa1
13th	ZnKa1	ZnKa1	ZnKa1	ZnKa1	ZnKa1	CuKa1
14th	CuKa1	CuKa1	CuKa1	CuKa1	CuKa1	ZnKa1
15th	PbLa1	PbLa1	PbLa1	PbLa1	PbLa1	PbLa1
16th	AsKa1	AsKa1	AsKa1	AsKa1	AsKa1	AsKa1
17th	MnKa1	MnKa1	MnKa1	MnKa1	MnKa1	MnKa1
18th	NiKa1	NiKa1	NiKa1	NiKa1	NiKa1	NiKa1
19th	CrKa1	CrKa1	CrKa1	CrKa1	CrKa1	CrKa1

ppm Concentration Data

Break vs. Slip

Using the ppm concentration data, mean relative abundances for the elements of interest in the slipped surfaces and clean breaks were calculated for each type: variety. The tabulated means are listed in Tables 5 and 6 below.

Table 5. Mean concentrations (ppm) of the elements of interest in the slipped surfaces of sherds from each type: variety.

	Joventud Red	Sierra Red	Pital Cream	Flor Cream	Chunhinta Black	Polvero Black
CaKa1	28346.82	41806.79	25753.06	28031.86	31938.1	35178.37
BaLa1	770.3873	788.3526	1445.437	440.8572	681.0838	714.2521
TiKa1	4990.621	4538.321	4995.882	4847.949	5151.177	4773.973
CrKa1	-83.2987	-64.3967	-178.44	-159.396	-170.453	-144.9
MnKa1	189.4982	186.2846	199.9285	196.1921	166.1413	200.7083
FeKa1	30992.43	28292.92	20172.93	19418.47	19127.99	19160.72
CoKa1	21.29635	15.98236	20.87834	15.6619	12.82951	12.41722
NiKa1	61.05672	53.64246	38.38586	32.40663	31.66865	45.252
CuKa1	40.44531	41.00317	26.25399	22.07214	26.15023	25.79882
ZnKa1	62.26892	60.26111	66.75293	44.92677	49.68761	38.35699
AsKa1	5.56787	5.923802	4.777103	3.999155	4.105793	3.944657
PbLa1	12.37992	12.02103	10.60691	10.84993	10.22797	10.35074
ThLa1	4.839231	4.691076	4.752026	4.561184	3.817076	3.413131
RbKa1	36.00498	33.21644	39.74615	35.71611	25.91158	19.36566
U La1	-7.0601	-6.39881	-6.67936	-5.18235	-5.11606	-5.82844
SrKa1	45.0265	41.22785	38.21535	34.90203	43.40712	33.84391
Y Ka1	23.63603	22.46865	24.45063	22.75132	19.11645	21.53129
ZrKa1	197.6835	168.0499	148.9016	143.1783	122.1487	110.3606
NbKa1	4.417971	4.324813	4.341951	4.373076	3.217347	3.144536
MoKa1	22.21811	21.52035	33.02124	34.61592	33.64576	34.56356
RhKa1	0	0	0	0	0	0
SnKa1	2.825149	2.748961	3.049285	3.025436	3.067006	3.083755
SbKa1	15.84395	14.48388	19.56227	19.19449	19.76462	20.1118

Table 6. Mean concentrations (ppm) of the elements of interest in the clean breaks of sherds from each type: variety.

	Joventud Red	Sierra Red	Pital Cream	Flor Cream	Chunhinta Black	Polvero Black
CaKa1	57315.76	72335.63	45148.2	38547.28	53402.51	59611.04
BaLa1	733.4074	768.9513	1074.717	488.5083	749.0163	638.3289
TiKa1	3982.462	3698.53	4618.998	4664.882	4745.972	4507.238
CrKa1	-73.5686	-71.829	-179.05	-183.584	-189.002	-180.637
MnKa1	253.2535	266.771	204.3288	219.2698	171.8851	209.5561
FeKa1	26659.44	23136.3	17047.99	15714.69	15266.58	13740.16
CoKa1	16.56207	13.58819	15.26536	12.43608	10.74514	9.925938
NiKa1	31.14934	30.01439	14.55032	14.1499	15.07687	19.81941
CuKa1	43.7823	42.93894	24.48619	27.84492	25.97258	27.32559
ZnKa1	52.1201	47.67366	42.0637	38.80356	35.39246	30.58097
AsKa1	4.797879	5.46473	3.73508	3.704551	3.64712	3.73766
PbLa1	11.57963	11.40926	10.23974	10.18884	9.586011	9.63446
ThLa1	4.632269	4.431472	4.523014	4.135004	3.495226	3.149198
RbKa1	32.87804	30.15023	38.31859	31.19306	23.13936	17.7447
U La1	-5.99301	-5.87312	-5.72055	-5.10101	-5.15073	-5.85009
SrKa1	54.15234	46.84041	39.28967	36.28763	41.418	30.65797
Y Ka1	23.58263	22.87374	23.67997	21.58317	18.39879	20.39601
ZrKa1	168.0239	146.6654	125.5161	114.9345	97.51482	89.62397
NbKa1	4.49977	4.30099	4.184722	3.951063	2.913132	2.825996
MoKa1	24.06158	23.51534	37.17573	39.63694	40.61692	41.38928
RhKa1	0	0	0	0	0	0
SnKa1	2.850707	2.775882	3.166057	3.170494	3.292468	3.335932
SbKa1	16.48315	14.99322	21.94899	21.65231	24.05138	24.93444

The differences between the mean concentrations of each element in the clean breaks and slipped surfaces were calculated again for the ppm data, as the calibration may affect the magnitude of the differences. For each element measured, the null hypothesis was that there would be no difference between the concentration in clean break and the concentration in the slipped surface. For calcium, titanium, manganese, iron, cobalt, nickel, zinc, arsenic, lead, zirconium, molybdenum, tin, and antimony, $p < 0.001$. For chromium, $p = 0.001$; for copper, $p = 0.003$; for thorium, $p = 0.019$; and for strontium, $p = 0.009$. Therefore, we can reject the null

hypothesis that there is no difference between the clean break and slipped surfaces' mean concentrations of these elements at the 95% confidence interval. This suggests that pXRF spectrometry was successfully isolated to the slipped surface for calcium, titanium, chromium, manganese, iron, cobalt, nickel, copper, zinc, arsenic, lead, thorium, strontium, zirconium, molybdenum, tin, and antimony when evaluating concentration at the ppm level using the Mudrock Trace Element calibration.

Once again, several sets of means were not significantly different. For barium, $p = 0.577$; for rubidium, $p = 0.352$; for uranium, $p = 0.053$; for yttrium, $p = 0.096$; and for niobium, $p = 0.444$. Therefore, we accept the null hypothesis that there is no difference between the clean break and slipped surfaces' mean concentrations of these elements at the 95% confidence interval. This suggests that pXRF analysis consistently extended past the slipped surface and into the underlying paste for barium, rubidium, uranium, yttrium, and niobium. Because of this, these five elements will be excluded from the following analysis. Rhodium will again be excluded from analyses as calibration revealed its only significant source was the pXRF unit itself. Chromium was also removed because the calibration consistently produced negative values for its concentration. These negative values are likely a result of Mudrock calibration not fully reflecting the composition of archaeological ceramics.

Determining Compositional Groups

Two-step cluster analysis was run with the concentrations of calcium, titanium, manganese, iron, cobalt, nickel, copper, zinc, arsenic, lead, thorium, strontium, zirconium, molybdenum, tin, and antimony as variables. Including all 16 elements in the analysis produced five poor-to-fair-quality clusters (Figure 7). The number of elements included was reduced based

on predictor variable importance. Only those elements with a predictor importance value of 0.5 or greater were kept, leaving calcium, iron, lead, thorium, zirconium, molybdenum, tin, and antimony as variables for further cluster analysis.

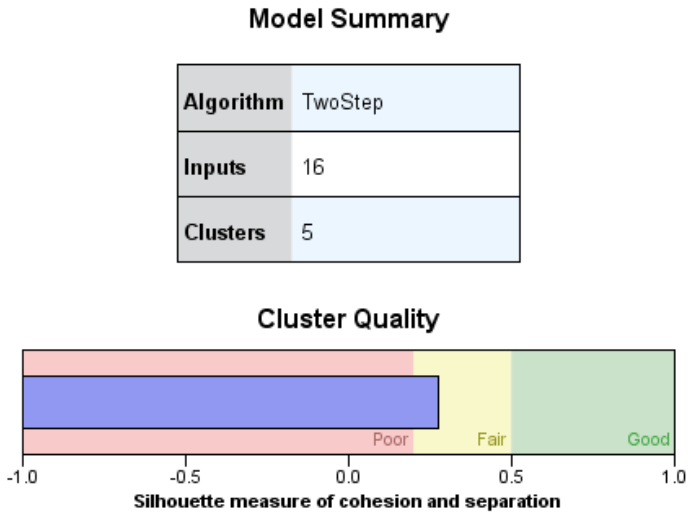

Figure 7. Model summary for the first cluster analysis, showing the number of elements included (inputs), the number of clusters produced, and the cluster quality.

The second cluster analysis produced two fair-quality clusters, and also indicated that thorium and calcium significantly lower predictor importance values than the other remaining variables. Thus, thorium and calcium were removed for the third cluster analysis. This also produced two fair-quality clusters, though their quality was higher than before. Lead was the least important for predicting group membership (the predictor importance for lead was 0.49, while the predictor importance for all other elements was greater than 0.50) and was thus removed from further analysis.

The fourth and final cluster analysis produced two fair-to-good quality clusters (Figure 8). 59.9% of slipped surfaces belonged to Group 1, and 40.1% belonged to Group 2. Molybdenum, tin, iron, antimony, and zirconium concentrations – in that order – predicted group membership.

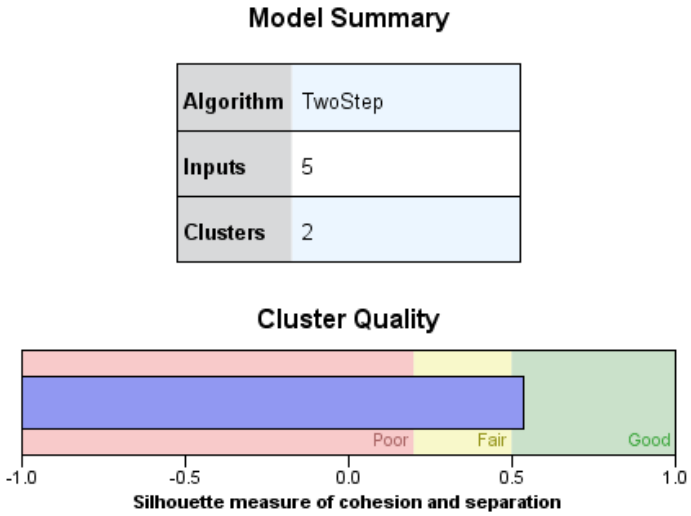

Figure 8. Model summary for the final cluster analysis, showing the number of elements included (inputs), the number of clusters produced, and the cluster quality.

Chi-squared tests of association revealed a strong relationship between group membership and slip color. As $p < 0.001$, there was less than a 0.1% chance that we would see the proportions of each slip color assigned to each compositional group by random chance if the proportions were equal. As seen in Table 7, 98.5% of cream-slipped sherds and 97.7% of black-slipped sherds belonged to Group 1. 84.7% of red-slipped sherds belonged to Group 2. These overarching trends in slip color apply to both type: varieties of the same color as well (Table 8).

100% of Pital Cream sherds, 97.8% of Flor Cream sherds, 97.0% of Chunhinta Black sherds, and 99.0% of Polvero Black sherds belonged to Group 1. 83.1% and 86.6% of Joventud Red and Sierra Red sherds, respectively, belonged to Group 2. Once again, $p < 0.001$, indicating there was less than a 0.1% chance that we would see the proportions of each type: variety assigned to each compositional group by random chance if the proportions were equal.

Table 7. Results of the chi-square test of association for slip color vs. compositional group assignment.

			TwoStep Cluster Number		
			1	2	Total
Slip Color	**Red**	Count	43	238	281
		Expected Count	168.3	112.7	281.0
		% within Color	15.3%	84.7%	100.0%
		Standardized Residual	-9.7	11.8	
	Cream	Count	64	1	65
		Expected Count	38.9	26.1	65.0
		% within Color	98.5%	1.5%	100.0%
		Standardized Residual	4.0	-4.9	
	Black	Count	259	6	265
		Expected Count	158.7	106.3	265.0
		% within Color	97.7%	2.3%	100.0%
		Standardized Residual	8.0	-9.7	
Total		Count	366	245	611
		Expected Count	366.0	245.0	611.0
		% within Color	59.9%	40.1%	100.0%

Table 8. Results of the chi-square test of association for type: varieties vs. compositional group assignment.

			TwoStep Cluster Number		
			1	2	Total
Type: Variety	**Joventud**	Count	26	128	154
		Expected Count	92.2	61.8	154.0
		% within Type: Variety	16.9%	83.1%	100.0%
		Standardized Residual	-6.9	8.4	
	Sierra	Count	17	110	127
		Expected Count	76.1	50.9	127.0
		% within Type: Variety	13.4%	86.6%	100.0%
		Standardized Residual	-6.8	8.3	
	Pital	Count	19	0	19
		Expected Count	11.4	7.6	19.0
		% within Type: Variety	100.0%	0.0%	100.0%
		Standardized Residual	2.3	-2.8	
	Flor	Count	45	1	46
		Expected Count	27.6	18.4	46.0
		% within Type: Variety	97.8%	2.2%	100.0%
		Standardized Residual	3.3	-4.1	
	Chunhinta	Count	163	5	168
		Expected Count	100.6	67.4	168.0
		% within Type: Variety	97.0%	3.0%	100.0%
		Standardized Residual	6.2	-7.6	
	Polvero	Count	96	1	97
		Expected Count	58.1	38.9	97.0
		% within Type: Variety	99.0%	1.0%	100.0%
		Standardized Residual	5.0	-6.1	
Total		Count	366	245	611
		Expected Count	366.0	245.0	611.0
		% within Type: Variety	59.9%	40.1%	100.0%

The association between a slipped surface's compositional group membership and the architectural group where it was excavated was evaluated using a chi-squared goodness-of-fit test. To generate expected proportions, all red slips were assumed to belong to Group 2 and all

cream and black slips were assumed to belong to Group 1. Table 9 shows the expected proportion of slips belonging to each compositional group by architectural group.

Table 9. Expected proportions of compositional group membership for slips excavated from each architectural group.

	Group 1	Group 2
Group A	59%	41%
Group B	68%	32%
Group C	41%	59%
Group F	70%	30%
Holtun West	32%	68%

The chi-squared goodness-of-fit test compared these expected proportions to those that were observed. For Group A, $p = 0.140$; for Group B, $p = 0.364$; for Group C, $p = 0.024$; for Group F, $p = 0.593$; and for Holtun West, $p = 0.082$. Therefore, at the 95% confidence interval, the only significant difference in the expected and observed compositional group assignments was for Group C. A second set of chi-square tests of association were run to evaluate this relationship. In these tests, $p < 0.001$ for slip color vs. group membership and type: variety vs. group membership, indicating that there was less than a 0.1% chance that we would see the proportions assigned to each group by random chance if the proportions were equal. 88.5% of red slips belong to Group 2, while 100% of cream and black slips belonged to Group 1 (Table 10). When factoring in individual type: varieties, once again 100% of Pital Cream, Flor Cream, Chunhinta Black, and Polvero Black sherds belonged to Group 1. 86.1% of Joventud Red and 89. 4% of Sierra Red sherds belonged to Group 2 (Table 11). From this, we can see the significant difference in expected and observed compositional group membership was the result of an increased correlation between slip color and group membership for sherds excavated in Group C.

Table 10. Results of the chi-square test of association for type: varieties vs. compositional group assignment of sherds excavated in Group C.

			TwoStep Cluster Number		
			1	2	Total
Slip Color	**Red**	Count	15	115	130
		Expected Count	63.0	67.0	130.0
		% within Color	11.5%	88.5%	100.0%
		Standardized Residual	-6.0	5.9	
	Cream	Count	23	0	23
		Expected Count	11.1	11.9	23.0
		% within Color	100.0%	0.0%	100.0%
		Standardized Residual	3.6	-3.4	
	Black	Count	70	0	70
		Expected Count	33.9	36.1	70.0
		% within Color	100.0%	0.0%	100.0%
		Standardized Residual	6.2	-6.0	
Total		Count	108	115	223
		Expected Count	108.0	115.0	223.0
		% within Color	48.4%	51.6%	100.0%

Table 11. Results of the chi-square test of association for type: varieties vs. compositional group assignment of sherds excavated in Group C.

			TwoStep Cluster Number		
			1	2	Total
Type: Variety	**Joventud**	Count	5	31	36
		Expected Count	17.4	18.6	36.0
		% within Type: Variety	13.9%	86.1%	100.0%
		Standardized Residual	-3.0	2.9	
	Sierra	Count	10	84	94
		Expected Count	45.5	48.5	94.0
		% within Type: Variety	10.6%	89.4%	100.0%
		Standardized Residual	-5.3	5.1	
	Pital	Count	5	0	5
		Expected Count	2.4	2.6	5.0
		% within Type: Variety	100.0%	0.0%	100.0%
		Standardized Residual	1.7	-1.6	
	Flor	Count	18	0	18
		Expected Count	8.7	9.3	18.0
		% within Type: Variety	100.0%	0.0%	100.0%
		Standardized Residual	3.1	-3.0	
	Chunhinta	Count	21	0	21
		Expected Count	10.2	10.8	21.0
		% within Type: Variety	100.0%	0.0%	100.0%
		Standardized Residual	3.4	-3.3	
	Polvero	Count	49	0	49
		Expected Count	23.7	25.3	49.0
		% within Type: Variety	100.0%	0.0%	100.0%
		Standardized Residual	5.2	-5.0	
Total		Count	108	115	223
		Expected Count	108.0	115.0	223.0
		% within Type: Variety	48.4%	51.6%	100.0%

Characteristics of Compositional Groups

The distinguishing chemical characteristics of each cluster can be seen in the bivariate plots in Figures 9 through 12, the box-and-whisker plot in Figure 13, and descriptive statistics in Table 12.

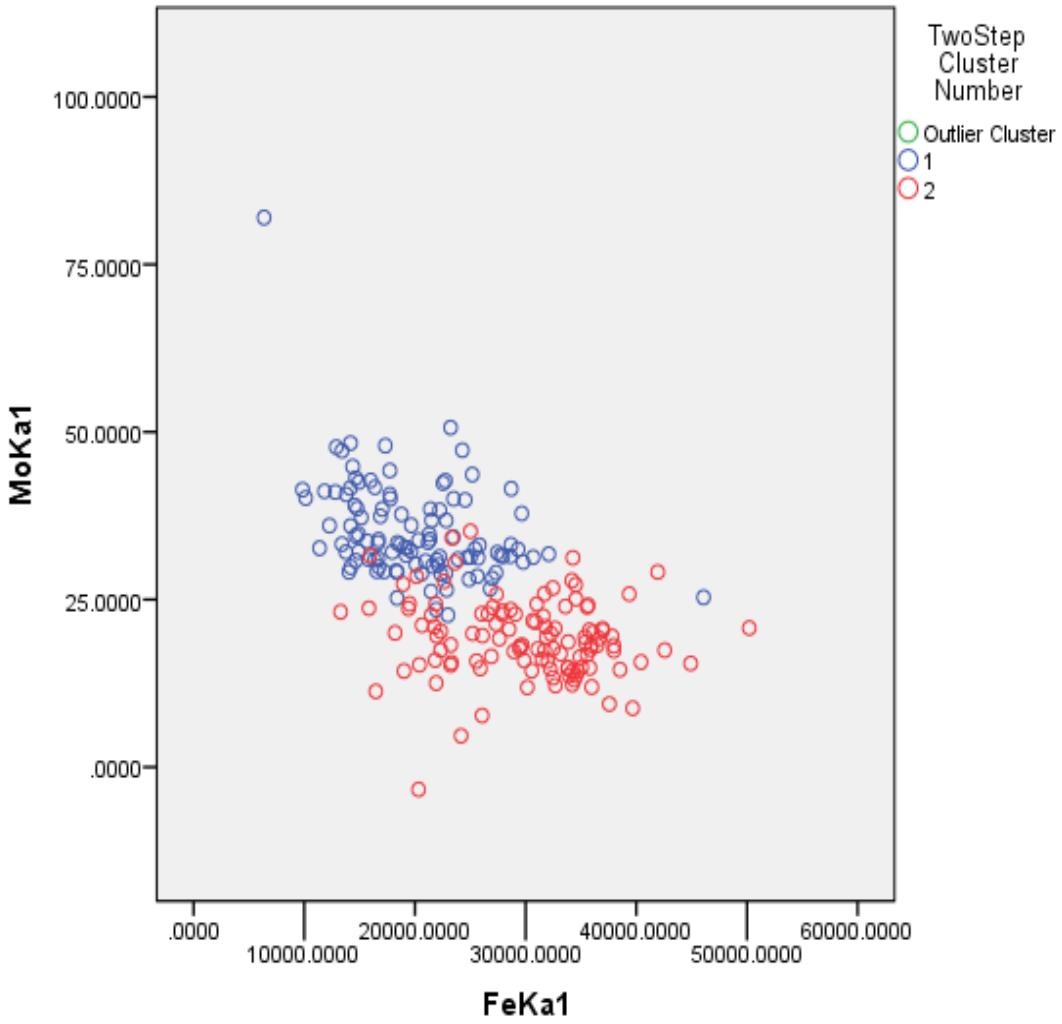

Figure 9. Bivariate plot showing the differences in compositional groups in terms of molybdenum vs. iron concentrations (ppm).

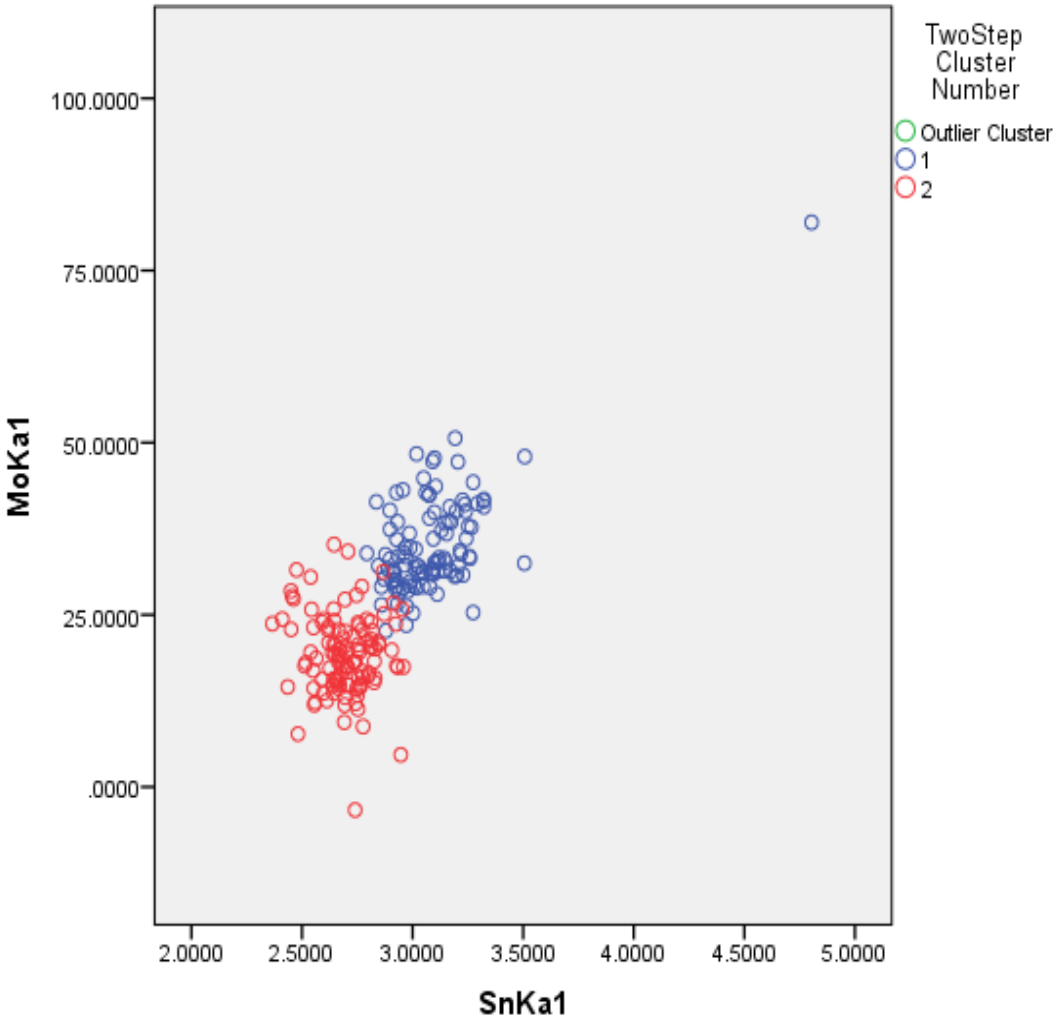

Figure 10. Bivariate plot showing the differences in compositional groups in terms of molybdenum vs. tin concentrations (ppm).

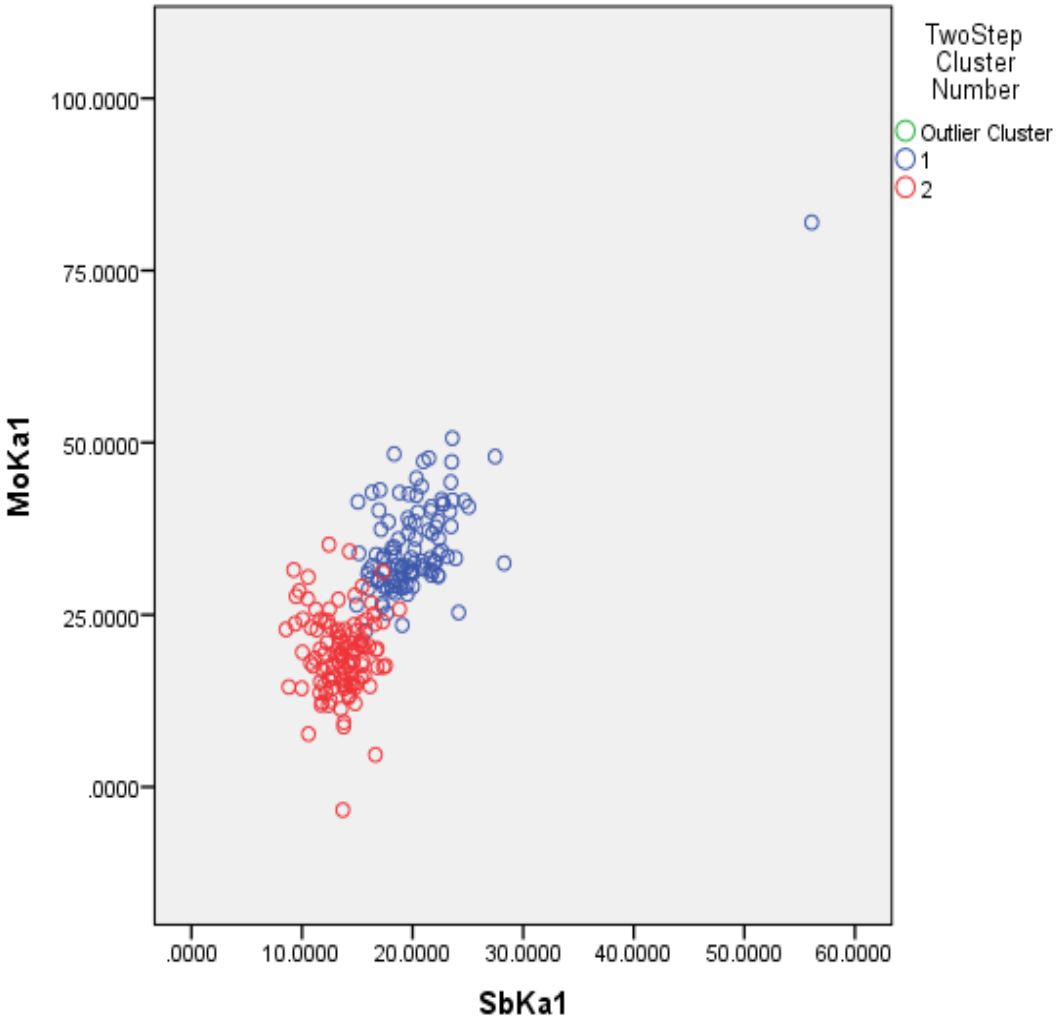

Figure 11. Bivariate plot showing the differences in compositional groups in terms of molybdenum vs antimony concentrations.

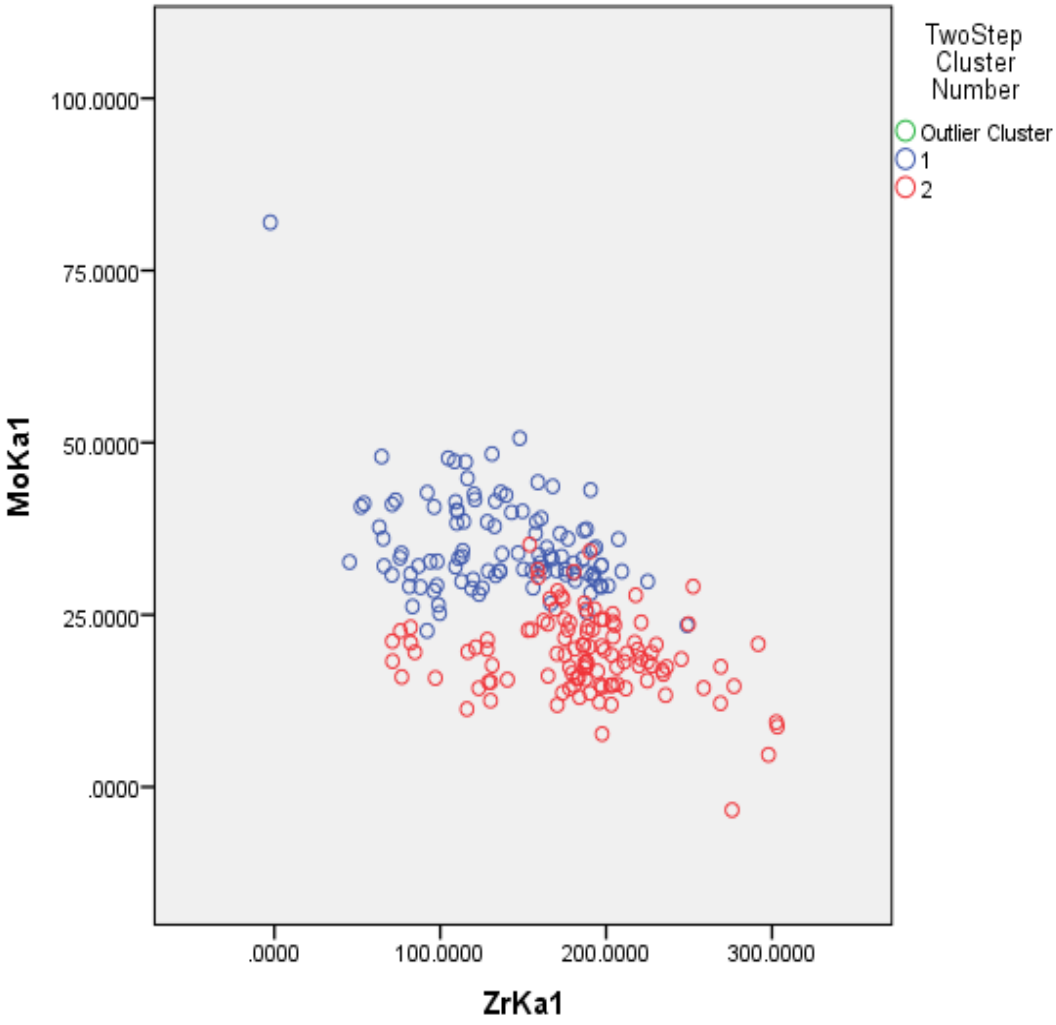

Figure 12. Bivariate plot showing the differences in compositional groups in terms of molybdenum vs. zirconium concentrations (ppm).

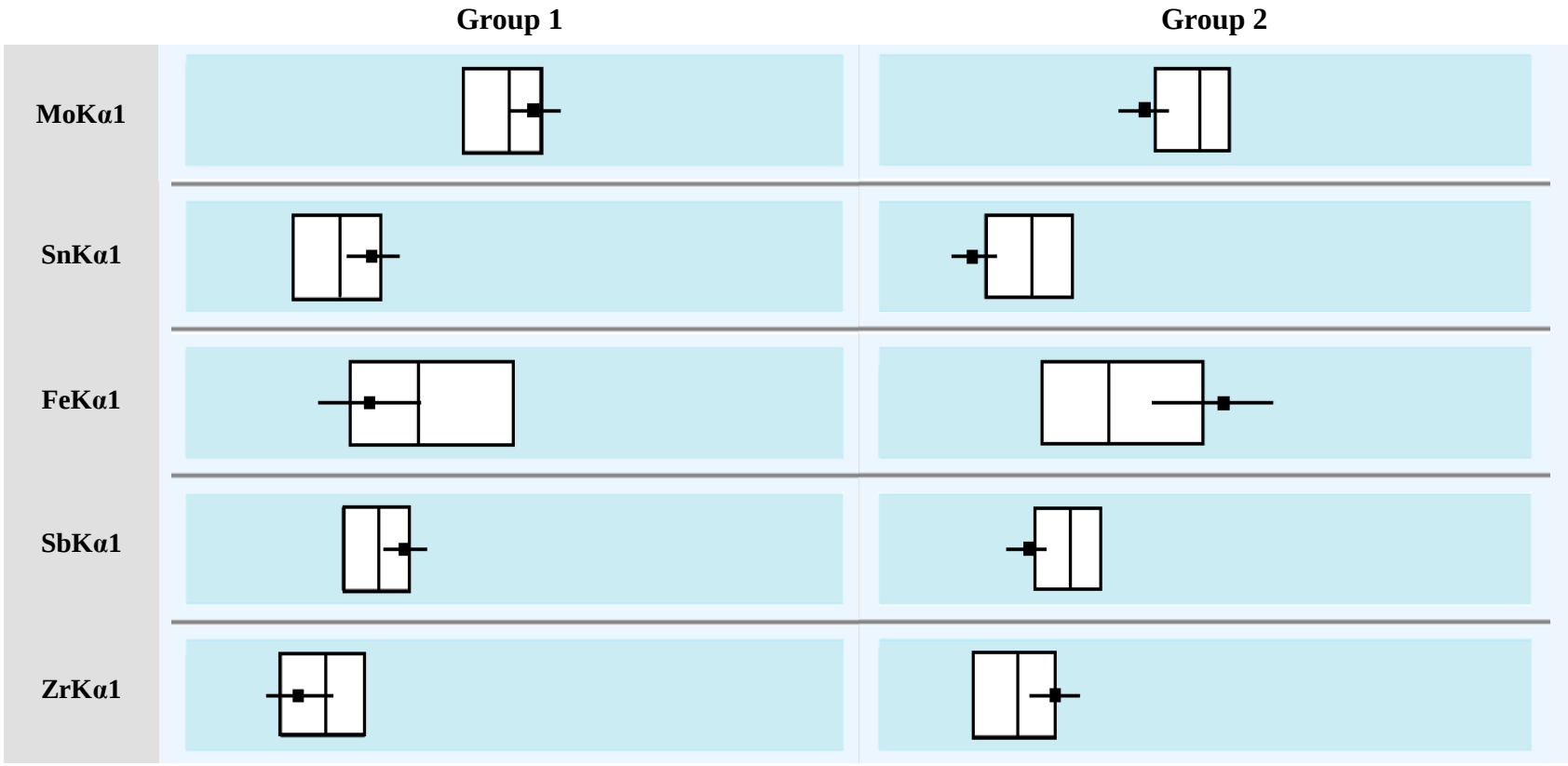

Figure 13. Box-and-whisker plots showing the different means and distributions for concentrations of molybdenum, tin, iron, antimony, and zirconium in the two compositional groups (box-and-whisker plots for different elements are not on the same scale).

Table 12. Mean concentrations and standard deviations in concentrations of iron, zirconium, molybdenum, tin, antimony in the compositional groups.

	Group 1		Group 2	
	Mean	Standard Deviation	Mean	Standard Deviation
Fe	19771.88 ppm	5284.357 ppm	30523.08 ppm	6940.623 ppm
Zr	122.8143 ppm	47.07653 ppm	193.7831 ppm	71.75341 ppm
Mo	34.19975 ppm	7.39832 ppm	19.84675 ppm	6.872978 ppm
Sn	3.087476 ppm	0.229766 ppm	2.71699 ppm	0.13513 ppm
Sb	20.23469 ppm	4.475639 ppm	13.87533 ppm	2.432947 ppm

Group 1 is marked by higher-than-average concentrations of molybdenum, tin, and antimony. Concentrations of iron and zirconium are lower-than-average. These trends are reversed for Group 2: molybdenum, tin, and antimony are found in lower-than-average concentrations and iron and zirconium in higher-than-average ones. Within each group, the least variation in concentration was seen in tin and antimony, while the highest variation is seen in iron.

Summary

pXRF spectrometry consistently distinguished between the slip and underlying paste for most elements of interest. This ability was used to determine two distinct compositional groups based on slip. Group 1 consists of cream and black slips. Compositionally, these slips have 14,487.52 ppm to 25,056.23 ppm iron, 75.74 ppm to 169.89 ppm zirconium, 26.80 ppm to 41.60 ppm molybdenum, 2.86 ppm to 3.32 ppm tin, and 15.76 ppm to 24.71 ppm antimony. This makes them comparatively high in molybdenum, tin, and antimony, while comparatively low in iron and zirconium. Group 2 consists of red slips. Compositionally, these slips have 23,582.46 ppm to 37,463.71 ppm iron, 122.03 ppm to 265.54 ppm zirconium, 12.97 ppm to 26.72 ppm molybdenum, 2.58 ppm to 2.85ppm tin, and 11.44 ppm to 16.31 ppm antimony. This makes

them comparatively high in iron and zirconium, while comparatively low in molybdenum, tin, and antimony. The concentrations of other elements present in the slips were variable and thus do not follow significant trends within these compositional groups. No significant differences were observed based on time period (Middle or Late Preclassic-period slips of a given color), nor based on the architectural groups from which the sherds were excavated. The significance of the detected compositional groups and what they imply about the production of ceramic slips during the Preclassic period is discussed in the next chapter.

CHAPTER 5: CONCLUSION

The research in this thesis was carried out with several major experimental hypotheses, one concerning methodology and the other three concerning chemical compositions of the slips. The methodological hypothesis was that pXRF spectrometry would be an appropriate and successful technique for chemical characterization studies of ceramic slips. The hypotheses concerning chemical compositions were that significant, detectable differences would be seen between 1) each slip color; 2) the two different type: varieties of each slip color, which reflect change over time; and 3) sherds excavated in different architectural groups.

Statistical analyses of the data indicate that pXRF spectrometry is suitable for chemical characterization studies of ceramic slips. They also yielded two compositional groups with a strong correlation to slip color. This indicates that red slips were significantly different from cream and black slips. No significant differences were seen based on the time period during which the slips were produced or the architectural groups where they were excavated. Thus, the data and statistical analyses support the methodological hypothesis and the first compositional hypothesis, but not the second and third compositional hypotheses.

The remainder of this chapter interprets the results in greater detail in order to evaluate their significance. It then explores the implications of the results for future research. These implications focus on chemical characterization studies of ceramic slips using pXRF spectrometry, further analysis of the sample to augment and improve the results, and analysis of Middle and Late Preclassic-period red, cream, and black slips overall.

pXRF Spectrometry as a Technique for the Chemical Characterization of Ceramic Slips

Isolating Analyses to the Slip

Clean breaks represent a multilayer combination of the slipped surface, the paste, and any zones of interaction. pXRF spectrometry being isolated to the slipped surfaces and not extending into the paste would result in different elemental data being generated for the slipped surfaces and the clean break. Comparisons between the mean relative abundance of each element of interest for slipped surfaces and clean breaks showed that pXRF spectrometry yielded significantly different results when analyzing slipped surfaces versus clean breaks. Comparisons between the mean ppm concentrations of each element for slipped surfaces and clean breaks showed the same. For both types of data, there were cases were the elemental compositions of slipped surfaces and clean breaks were not significantly different. For the relative abundances, this made barium, titanium, and zirconium unanalyzable. For the calibrated ppm concentrations, barium, rubidium, uranium, yttrium, and niobium were unanalyzable. The difference in the sets of unanalyzable elements is a result of calibration affecting the magnitude of similarities and differences between means.

Where no significant difference was detected between the elemental concentrations in the slipped surfaces and clean breaks, the elements of concern tend to be among the heaviest elements of interest. These elements have the highest depth of penetration, making it more difficult for the x-ray beam to be isolated to the slip. However, this was not a universal problem for heavy elements, suggesting that slip is usually significantly thick for the analysis of elements of interest with pXRF spectrometry. The results suggest that the accurate analysis of the amount of barium in slips alone may never be possible, but for the other elements of concern, the use of a specific calibration may impact whether they can be accurately measured.

Types of Data

When analyzing the ROI data in terms of ranked relative abundances, iron and cobalt were marked as the most likely elements to distinguish between compositional groups. Cobalt, however, was not a significant factor in distinguishing between compositional groups, regardless of slip color. Molybdenum, tin, and antimony were also noted as possible candidates for distinguishing between compositional groups, though their predictor importance values were not expected to be as strong as iron and cobalt. Zirconium was excluded from ROI analyses. Such deviations from prediction stem from calibration affecting the magnitude of differences in the concentrations of each element.

The differences between the types of data indicate that relative abundances in the form of ROI data can give an idea of key predictor elements for compositional groups – and, thus, overall differences in composition between slips – but fully-quantitative calibrated data is necessary to accurately determine what elements would define compositional groups. On the other hand, relative abundance data may be used to assess compositional group membership when the compositional groups are already known.

Chemical Characterization of the Slips in This Study

Comparing Compositional Groups in Terms of Slip Color

Based on the compositional groups determined by cluster analyses, red slips were significantly different from black and cream slips in terms of their concentrations of iron, zirconium, molybdenum, tin, and antimony. Of these elements, iron was the most abundant, zirconium was the second-most abundant, molybdenum was the third-most abundant, antimony the fourth-most abundant, and tin the fifth-most abundant within all slips, regardless of color or

whether the slip was on the exterior or interior of the vessel. The red slips had higher-than-average concentrations of iron and zirconium and lower-than-average concentrations of molybdenum, tin, and antimony. The opposite trends applied for black and cream slips.

There are explanations for the distinct compositional groups that are not related to intentional choices by the potter during vessel production. What materials were being stored inside a vessel, for example, could alter the concentrations of elements detected on the interior slip, while the deposition conditions can further affect the compositions of any exposed surfaces of a sherd. In such cases there would be higher variability between the concentrations of elements in interior and exterior surfaces. However, the consistencies between interior and exterior slips and strong correlation between group membership and slip color suggest that the differences in iron, zirconium, molybdenum, tin, and antimony concentrations between compositional groups were due to the manufacturing process as opposed to being effects of use and deposition.

Of the key predictor elements for compositional groups, differences in iron concentration have the most predictable effects on slip color. The oxidation of iron results in red, orange, or yellow colors in fired clays. (Shephard 1956; Rice 1987). The higher concentration of iron in red slips is thus heavily responsible for their color. The analyses also reveal that red and black slips were compositionally distinct, rather than the same slip fired in different atmospheres to achieve the desired color. The effect of tin may also have a clear correlation to color. Throughout the world, tin has frequently been employed in glazes to produce an opaque, white surface (see, for example, Molera et al. 2001; Rauschenberg 2005; Ortega Feliu et al. 2018). This indicates that the higher tin concentrations in cream and black slips may result in a white- or whitish-pink base color for the slip. Additions of antimony may result in a slightly yellow color, as antimony has

been used in ceramics to create yellow pigments that are applied on top of tin glazes (Molera et al. 2001, Rauschenberg 2005). The roles of zirconium and molybdenum in determining slip color are less predictable.

Cream and black slips were not distinguished in the compositional groups indicated by fair-to-good-quality clusters. Yet color indicates that there were differences in slip recipes or manufacturing processes that pXRF spectrometry was not able to distinguish. One of the most common colorants in black and grey slips is iron fired in a reducing atmosphere (Shepard 1956; Rice 1987). It is possible that the cream slips were fired in an oxidizing atmosphere – potentially leading to the yellow or pinkish hue of Pital Cream slips – and the black slips were fired in a reducing atmosphere. It is also possible that the black slips contained high quantities of carbonaceous material or were smudged to achieve the black color. Since carbon cannot be measured by pXRF spectrometry, this may be the main element that distinguishes the cream and black slips. The latter option is suggested by sherds that have an oxidized (red, orange, or yellow paste) but a black slip. A slip that is greyer in color with an underlying black or grey paste suggests a reducing atmosphere.

Elements Not Reflected by Compositional Group

To achieve fair-to-good quality for compositional group fit, numerous elements were removed from analyses. These elements were calcium, titanium, chromium, manganese, cobalt, nickel, copper, zinc, arsenic, lead, thorium, and strontium. Each of these element's differences in concentration did not cleanly cohere to either compositional group, indicating that they did not play a significant role in distinguishing between red vs. black and cream slips overall. Where lighter elements, particularly calcium, are concerned, it may also indicate lesser sensitivity in

pXRF, as calcium concentrations are frequently revealed to be important elements in INAA analyses of ceramics (see, for examples, Callaghan et al. 2017).

However, there are possible explanations for the wide variation in the concentrations of elements of interest. Use and deposition conditions may have introduced additional quantities of some elements to the slipped surfaces of individual vessels. Additionally, differences in the concentrations of some elements may reflect variation within slip colors rather than between them. This could indicate potters were using different clays or additives due to experimentation or availability of raw materials. It could also indicate that higher variation in the concentrations of these elements than the concentrations of iron, zirconium, molybdenum, tin, and antimony within a single clay source. The extent of the variation in the concentrations of these elements may be what separates Middle and Late Preclassic-period slips of each color.

Implications for Future Research

Improving the Quality of Sample Data

For the sherds in this study, additional pXRF spectrometry analyses can be undertaken to improve the data and potentially reveal further chemical distinctions between different slip colors and even type: varieties. Runs can be optimized for the analysis of lighter elements, such as calcium. This would require creating an atmosphere of 0 psi by conducting analyses under a vacuum or by flushing the unit with helium (see Hunt and Speakman 2015 for an example of using helium for the analysis of lighter elements). It would also not require the TiAl filter used in this thesis. Exact energy settings vary by calibration. To compliment the data produced in this thesis, Bruker's Mudrock major elements calibration would be used. However, if one were to use a different calibration for trace elements, the corresponding calibration and its analysis

conditions should be used for major element (i.e. optimized lighter element) analysis. Calibrations that are designed specifically for archaeological ceramics can be used, such as that developed by the Center for Applied Isotope Studies at the University of Georgia (Hunt and Speakman 2015). Alternatively, researchers can create their own calibrations to better quantify the data.

Additionally, the sherds in this sample can be analyzed with LA-ICP-MS. This is another suitable technique for surface analysis that may produce higher-quality quantitative data, though it lacks pXRF spectrometry's advantages of portability, degree of nondestructive-ness, and relative affordability. LA-ICP-MS analysis would be able to confirm the compositional groups, as pXRF spectrometry was able to identify compositional groups previously determined by LA-ICP-MS in Ferguson et al.'s 2015 study, and it could potentially detect any compositional differences pXRF spectrometry could not detect.

Differentiating the Chemical Compositions of Cream and Black Slips

While the number of sherds in the sample represented 10% of the sherds of each type: variety of interest excavated at Holtun in 2017, the number sherds of each type: variety was not equal. Significantly fewer cream-slipped sherds were excavated in the 2017 season than red- and black slipped ones. This led to only 10 Pital Cream and 23 Flor Cream sherds being in the sample. From here, only 65 cream-slipped surfaces were analyzed due to one Pital sherd having slip on only the exterior surface. Analyzing more cream-slipped sherds could reveal compositional differences between cream and black slips that were previously undetectable because of sample size.

Implications for Clay Sourcing and Ceramic Production at Holtun and Other Sites

Previous research on ceramic pastes at Holtun determined that slipped serving ware was locally-made and the raw materials were locally sourced. (Callaghan et al. 2017). If ceramic production of slipped serving ware occurred at the site, the slips would then be locally made, and their raw materials were likely locally sourced as well. The results of this thesis suggest that at least two different clay sources were used in creating Preclassic-period slips at Holtun: one for red slips and another for black and cream slips. Analysts may be able to identify the clay deposits from which the clays used to make these slips were sourced by analyzing raw clay samples with pXRF spectrometry under the same conditions used on the sherds. The source for red slips would have 23,582.46 ppm to 37,463.71 ppm iron, 122.03 ppm to 265.54 ppm zirconium, 12.97 ppm to 26.72 ppm molybdenum, 2.58 ppm to 2.85ppm tin, and 11.44 ppm to 16.31 ppm antimony. The source for the black and cream slips, on the other hand, would have 14,487.52 ppm to 25,056.23 ppm iron, 75.74 ppm to 169.89 ppm zirconium, 26.80 ppm to 41.60 ppm molybdenum, 2.86 ppm to 3.32 ppm tin, and 15.76 ppm to 24.71 ppm antimony. Finding such deposits of clay would verify that sherds were locally-produced. If multiple deposits had these concentrations of iron, zirconium, molybdenum, tin, and antimony, but varying amounts of other elements, it may explain the variable concentrations of calcium, titanium, chromium, manganese, cobalt, nickel, copper, zinc, arsenic, lead, thorium, and strontium in slips of the same color. If deposits matching the iron, zirconium, molybdenum, tin, and antimony cannot be found, this would indicate more mixing and processing of raw clays were involved in the slip recipes.

With the data used in this thesis, the further statistical tests can be undertaken to evaluate any relationships between vessel form and slip composition. This could reveal any relationships between specific slip recipes used on specific forms, which may reveal a connection between slip

composition and vessel function. Combining this with datasets generated from runs optimized for light elements and/or clay sources can further our understandings of ceramic production, specialization, and standardization.

The data produced in this study suggest some amount of standardization in the production of ceramic slips. Whether as a byproduct of available raw materials; consumer preferences; or finding the best, easiest, or only method that worked to produced a slip of a given color to be applied over the corresponding pastes, potters at Holtun seem to have found a method that worked and used it across the site. This small indication of standardization in craft production needs to be expanded on by more research on ceramics (including the pastes) and other materials produced at Holtun.

The pXRF analysis procedures could be repeated on red-, black-, and cream-slipped Flores Waxy Ware and Paso Caballo Waxy Ware sherds from other sites to determine their slip compositions and to source the raw materials used to make them. Such studies would allow for site-to-site comparison of slip recipes and any inter-site variability between them. This could increase our understanding of the extent to which information about ceramic production was shared between sites, revealing to what degree slip recipes were standardized in the region and to what degree potters experimented.

Chi-square tests of association revealed that there was no significant difference between slips of the same color during the Middle versus Late Preclassic periods. This supports Forsyth's (1989) argument that divisions between the Flores Waxy Ware and Paso Caballo Waxy Ware are arbitrary. Nonetheless, trends in hue and shade – as well as forms, a subject untouched on in this research – that differentiate Middle and Late Preclassic-period red- and cream-slipped type: varieties should not be entirely discarded at this point. Intra-type: variety variability in all

elements should be assessed. This would determine if the amount of variability in chemical composition was consistent between time periods. Furthermore, the true difference between Middle and Late Preclassic-period slips may stem not from major, consistent differences in elemental concentrations, but in the extent to which slip recipes for a given color differ from each other in each period. Beyond chemical composition, postfiring techniques such as polishing can make slip colors darker and brighter (Shephard 1956; Rice 1987). The consistent use of such practices may also distinguish between Middle and Late Preclassic period slips. Finally, compositional differences in the pastes and temper need to be assessed, since ceramic type: varieties, wares, and traditions are based on more than slip alone.

Summary

Data analysis revealed that pXRF spectrometry was a suitable analysis technique for the chemical characterization of ceramics slips as analysis could be restricted to the topmost layer of the sherd. This mirrors the success Bezur and Casadio (2012) and al-Saad (2002) have found using pXRF spectrometry on glazes. The results obtained with the method can be strengthened by running a second set of sets for major elements under optimized conditions for their detection, using calibrations specifically designed for archaeological ceramics, and conducting LA-ICP-MS analyses on the same samples for comparison.

pXRF spectrometry was able to distinguish consistent compositional differences between iron, zirconium, molybdenum, tin, and antimony in red slips versus black and cream slips. Black and cream slips were chemically indistinct in terms of these elements as a cohesive group, suggesting that they used the same slip recipes save for two possible differences that pXRF spectrometry cannot detect: 1) that cream slips were fired in an oxidizing atmosphere and black

slips in a reducing atmosphere and/or 2) that large amounts of carbonaceous material were added to the clay. Other elements were present in each slip, but their concentrations were highly variable. These elements should be analyzed further to determine if the degree of variation in them differs between type: varieties of the same color, thus reflecting trends in experimentation and standardization. They may also reflect compositional differences in clay within or between sources.

To explore the latter option, the results can also be used to source the clay used to create each type of slip. Previous research (Callaghan et al. 2017) on Preclassic-period pastes at Holtun suggests local production, so samples of clay near Holtun can be analyzed with pXRF spectrometry to see if their concentrations of iron, zirconium, molybdenum, tin, and antimony match the slips. Samples at other sites can also be analyzed to see if recipes for slips of each color were consistent throughout the region. Additionally, such research can expand upon our understanding of ceramic classifications.

Since pXRF is portable, non-destructive, and relatively affordable compared to other methods of chemical analysis, it makes chemical characterization studies more accessible. This successful application of pXRF to study ceramic slips can provide opportunities to explore questions about archaeological classifications, ceramic production, trade, and many other topics for the Maya area and other regions. These data can be especially useful for quick chemical characterizations to determine which questions and samples merit future analyses, as well as in cases where small pieces of material cannot be removed for sampling. As such, using pXRF spectrometry on ceramic slips greatly increases the amount of research that can be done and the amount of knowledge that can be gleaned.

APPENDIX: SAMPLE LIST WITH EXCAVATION OPERATION, TYPE: VARIETY, VESSEL FORM, AND MUNSELL VALUES

Table 13. Sample list with excavation operation, type: variety, vessel form, and Munsell values.

				Munsell Values		
	Operation	**Type: Variety**	**Vessel Form**	**Exterior**	**Interior**	**Clean Break**
HTN17001	HTN 2-29C-11-14	Joventud Red: Joventud Variety	Jar	10R 5/8	7.5R 5/8	7.5YR 6/3
HTN17002	HTN 2-29C-11-15	Joventud Red: Joventud Variety	Dish	7.5R 4/8	10R 4/8	5YR 6/6
HTN17003	HTN 2-29C-11-17	Joventud Red: Joventud Variety	Bowl	2.5YR 4/8	2.5YR 4/8	7.5YR 6/6
HTN17004	HTN 2-29C-11-17	Joventud Red: Joventud Variety	Dish	10R 4/8	10R 5/8	GLEY1 6/N
HTN17005	HTN 2-29C-11-5	Joventud Red: Joventud Variety	Tecomate	2.5YR 5/6	10R 5/6	5YR 6/4
HTN17006	HTN 2-29C-11-5	Joventud Red: Joventud Variety	Dish	2.5YR 5/6	2.5YR 5/6	7.5YR 5/4
HTN17007	HTN 2-29C-11-5	Joventud Red: Joventud Variety	Bowl	10R 4/8	10R 4/8	7.5YR 3/1
HTN17008	HTN 2-29C-12-11	Joventud Red: Joventud Variety	Bowl	7.5R 5/6	7.5R 4/6	7.5YR 6/3
HTN17009	HTN 2-29C-12-7	Joventud Red: Joventud Variety	Jar	10R 4/8	10R 5/8	5YR 6/6
HTN17010	HTN 2-29C-12-7	Joventud Red: Joventud Variety	Form Not Determined	10R 4/8	10R 4/8	7.5YR 6/4
HTN17011	HTN 2-29C-12-7	Joventud Red: Joventud Variety	Jar	10R 4/8	5YR 6/6	2.5Y 5/3
HTN17012	HTN 2-29C-12-7	Joventud Red: Joventud Variety	Jar	7.5R 4/8	7.5R 4/8	5YR 6/4
HTN17013	HTN 2-29C-12-7	Joventud Red: Joventud Variety	Jar	10R 4/8	10R 5/8	7.5YR 6/6
HTN17014	HTN 2-29C-12-7	Joventud Red: Joventud Variety	Dish	2.5YR 4/8	2.5YR 4/8	2.5YR 5/8
HTN17015	HTN 2-29C-12-8	Joventud Red: Joventud Variety	Form Not Determined	10YR 4/8	2.5YR 6/8	7.5YR 5/3

				Munsell Values		
	Operation	**Type: Variety**	**Vessel Form**	**Exterior**	**Interior**	**Clean Break**
HTN17016	HTN 2-29C-12-8	Joventud Red: Joventud Variety	Form Not Determined	10R 5/6	10R 5/8	7.5YR 6/4
HTN17017	HTN 2-29C-12-8	Joventud Red: Joventud Variety	Form Not Determined	10R 4/8	10R 4/8	10YR 5/2
HTN17018	HTN 2-29C-12-9	Joventud Red: Joventud Variety	Dish	5YR 6/4	10R 5/8	5YR 6/6
HTN17019	HTN 2-29C-12-9	Joventud Red: Joventud Variety	Jar	10R 4/8	7.5R 5/8	5YR 6/6
HTN17020	HTN 2-29C-12-9	Joventud Red: Joventud Variety	Dish	10R 4/8	10R 4/8	10YR 7/4
HTN17021	HTN 11-3A-7	Joventud Red: Joventud Variety	Dish	2.5YR 4/8	2.5YR 5/8	7.5YR 4/2
HTN17022	HTN 11-3A-9	Joventud Red: Joventud Variety	Tecomate	7.5YR 7/3	10R 4/8	2.5YR 5/6
HTN17023	HTN 11-8-7 (216-267cm)	Joventud Red: Joventud Variety	Plate	10R 4/6	7.5R 4/6	2.5YR 5/4
HTN17024	HTN 11-8-7 (216-267cm)	Joventud Red: Joventud Variety	Dish	2.5YR 4/6	2.5YR 3/4	7.5YR 5/4
HTN17025	HTN 11-8-7 (216-267cm)	Joventud Red: Joventud Variety	Dish	10R 4/6	10R 4/8	5YR 6/4
HTN17026	HTN 11-8-7 (216-267cm)	Joventud Red: Joventud Variety	Dish	10R 4/6	2.5YR 3/4	5YR 5/3
HTN17027	HTN 11-8-7 (216-267cm)	Joventud Red: Joventud Variety	Plate	10R 4/6	10R 4/8	7.5YR 6/4
HTN17028	HTN 11-8-7 (216-267cm)	Joventud Red: Joventud Variety	Bowl	10R 5/6	7.5R 4/8	7.5YR 7/4
HTN17029	HTN 11-9-5	Joventud Red: Joventud Variety	Dish	10R 4/8	10R 4/8	5YR 6/4
HTN17030	HTN 11-9-5	Joventud Red: Joventud Variety	Dish	10R 4/6	10R 4/8	10YR 3/1

				Munsell Values		
	Operation	**Type: Variety**	**Vessel Form**	**Exterior**	**Interior**	**Clean Break**
HTN17031	HTN 11-9-5	Joventud Red: Joventud Variety	Dish	10R 4/6	10R 4/6	7.5YR 4/2
HTN17032	HTN 11-9-5	Joventud Red: Joventud Variety	Dish	10R 4/4	10R 4/6	10YR 3/1
HTN17033	HTN 11-9-5	Joventud Red: Joventud Variety	Dish	10R 4/8	10R 4/8	7.5YR 6/4
HTN17034	HTN 11-9-5	Joventud Red: Joventud Variety	Dish	10R 4/8	10R 5/8	10YR 5/1
HTN17035	HTN 11-9-5	Joventud Red: Joventud Variety	Dish	2.5YR 4/8	2.5YR 4/8	5YR 4/2
HTN17036	HTN 11-9-5	Joventud Red: Joventud Variety	Dish	10R 4/6	10R 4/6	7.5YR 5/3
HTN17037	HTN 11-9-5	Joventud Red: Joventud Variety	Dish	10R 4/6	10R 4/6	10YR 2/1
HTN17038	HTN 11-9-5	Joventud Red: Joventud Variety	Dish	10R 5/6	10R 5/6	5YR 5/2
HTN17039	HTN 11-9-5	Joventud Red: Joventud Variety	Dish	2.5YR 4/6	2.5YR 4/8	5YR 4/6
HTN17040	HTN 14-10-3	Joventud Red: Joventud Variety	Bowl	10R 4/6	10R 4/8	2.5Y 3/1
HTN17041	HTN 14-12-4	Joventud Red: Joventud Variety	Dish	10R 4/8	10R 4/8	5YR 5/6
HTN17042	HTN 14-12-4	Joventud Red: Joventud Variety	Dish	10R 4/8	10R 4/6	2.5YR 5/8
HTN17043	HTN 14-12-4	Joventud Red: Joventud Variety	Jar	10R 5/8	10R 5/6	10YR 4/2
HTN17044	HTN 14-12-4	Joventud Red: Joventud Variety	Dish	5R 7/4	10R 4/8	2.5YR 5/6
HTN17045	HTN 14-12-4	Joventud Red: Joventud Variety	Dish	10R 4/6	2.5YR 4/8	5YR 5/8

				Munsell Values		
	Operation	**Type: Variety**	**Vessel Form**	**Exterior**	**Interior**	**Clean Break**
HTN17046	HTN 14-12-4	Joventud Red: Joventud Variety	Dish	10R 4/8	10R 5/8	7.5YR 5/4
HTN17047	HTN 14-12-4 (2)	Joventud Red: Joventud Variety	Dish	2.5YR 6/6	2.5YR 5/6	7.5YR 5/3
HTN17048	HTN 14-12-4 (2)	Joventud Red: Joventud Variety	Dish	2.5YR 4/8	10R 4/8	7.5YR 6/6
HTN17049	HTN 14-12-4 (2)	Joventud Red: Joventud Variety	Dish	10R 4/6	2.5YR 4/6	2.5YR 3/2
HTN17050	HTN 14-12-4 (2)	Joventud Red: Joventud Variety	Dish	10R 4/8	10R 6/6	5YR 5/6
HTN17051	HTN 14-12-4 (2)	Joventud Red: Joventud Variety	Dish	2.5YR 4/8	10R 4/8	2.5YR 5/6
HTN17052	HTN 14-4-5	Joventud Red: Joventud Variety	Jar	2.5YR 5/6	2.5YR 5/8	5YR 5/2
HTN17053	HTN 14-4-5	Joventud Red: Joventud Variety	Jar	10R 4/8	10R 4/6	2.5YR 5/6
HTN17054	HTN 14-4-5	Joventud Red: Joventud Variety	Jar	2.5YR 4/8	2.5YR 4/8	2.5YR 4/8
HTN17055	HTN 14-4-5	Joventud Red: Joventud Variety	Jar	2.5YR 5/6	2.5YR 5/6	2.5YR 5/4
HTN17056	HTN 14-6-5	Joventud Red: Joventud Variety	Jar	10R 4/8	10R 4/8	2.5YR 5/6
HTN17057	HTN 14-6-5	Joventud Red: Joventud Variety	Dish	10R 5/8	10R 5/8	5YR 5/6
HTN17058	HTN 14-8-4	Joventud Red: Joventud Variety	Cuspidor	10R 5/8	5YR 6/4	2.5YR 5/6
HTN17059	HTN 14-8-4	Joventud Red: Joventud Variety	Dish	2.5YR 4/6	2.5YR 4/6	2.5YR 4/8
HTN17060	HTN 20-3A-8	Joventud Red: Joventud Variety	Dish	10R 3/6	7.5YR 4/6	7.5YR 5/4

				Munsell Values		
	Operation	**Type: Variety**	**Vessel Form**	**Exterior**	**Interior**	**Clean Break**
HTN17061	HTN 20-3A-8	Joventud Red: Joventud Variety	Dish	10R 4/6	10R 5/6	2.5Y 3/2
HTN17062	HTN 20-3A-8	Joventud Red: Joventud Variety	Dish	10R 4/6	10R 5/6	7.5YR 6/4
HTN17063	HTN 20-3A-8	Joventud Red: Joventud Variety	Dish	10R 6/6	7.5YR 4/1	5YR 5/4
HTN17064	HTN 24-1-3	Joventud Red: Joventud Variety	Dish	10R 5/6	10R 5/6	GLEY1 4/N
HTN17065	HTN 25-1-3	Joventud Red: Joventud Variety	Dish	10R 4/6	10R 4/6	5YR 5/4
HTN17066	HTN 25-1-3	Joventud Red: Joventud Variety	Dish	2.5YR 4/6	2.5YR 4/4	10YR 3/2
HTN17067	HTN 25-1-3	Joventud Red: Joventud Variety	Plate	10R 4/6	10R 4/8	7.5YR 6/4
HTN17068	HTN 25-1-3	Joventud Red: Joventud Variety	Dish	2.5YR 4/6	10R 4/8	10YR 4/2
HTN17069	HTN 25-1-3	Joventud Red: Joventud Variety	Dish	10R 4/6	10R 4/8	10YR 4/2
HTN17070	HTN 25-1-3	Joventud Red: Joventud Variety	Plate	2.5YR 5/4	2.5YR 4/4	10YR 3/1
HTN17071	HTN 25-1-3	Joventud Red: Joventud Variety	Bowl	10R 4/6	10R 4/4	10YR 3/2
HTN17072	HTN 25-1-3	Joventud Red: Joventud Variety	Dish	10R 4/6	10R 4/6	2.5Y 3/1
HTN17073	HTN 25-1-3	Joventud Red: Joventud Variety	Dish	2.5YR 4/8	2.5YR 4/8	7.5YR 6/6
HTN17074	HTN 25-1-3	Joventud Red: Joventud Variety	Dish	10R 4/6	10R 4/4	7.5YR 5/4
HTN17075	HTN 25-1-3	Joventud Red: Joventud Variety	Dish	10R 4/6	10R 4/6	7.5YR 6/4

				Munsell Values		
	Operation	**Type: Variety**	**Vessel Form**	**Exterior**	**Interior**	**Clean Break**
HTN17076	HTN 25-1-3	Joventud Red: Joventud Variety	Plate	10R 4/6	10R 4/8	5YR 4/2
HTN17077	HTN 25-1-3	Joventud Red: Joventud Variety	Dish	2.5YR 5/8	2.5YR 5/8	5YR 5/4
HTN17078	HTN 2-29A-6-17	Sierra Red: Sierra Variety	Dish	10R 5/8	10R 5/8	7YR 6/4
HTN17079	HTN 2-29D-0-0	Sierra Red: Sierra Variety	Bowl	10R 4/8	10R 4/8	2.5YR 5/8
HTN17080	HTN 9-A-0	Sierra Red: Sierra Variety	Dish	10R 4/6	2.5YR 6/6	7.5YR 6/6
HTN17081	HTN 9-A-1	Sierra Red: Sierra Variety	Bowl	2.5YR 4/6	2.5YR 4/4	10YR 7/3
HTN17082	HTN 9-A-10	Sierra Red: Sierra Variety	Jar	2.5YR 6/4	10R 4/6	5YR 5/3
HTN17083	HTN 9-A-10	Sierra Red: Sierra Variety	Jar	10R 4/6	10R 4/6	10YR 3/1
HTN17084	HTN 9-A-10	Sierra Red: Sierra Variety	Jar	2.5YR 4/8	2.5YR 4/1	10YR 6/3
HTN17085	HTN 9-A-6-1	Sierra Red: Sierra Variety	Dish	10R 3/4	10R 4/6	10YR 2/1
HTN17086	HTN 9-A-7	Sierra Red: Sierra Variety	Dish	7.5R 4/6	7.5R 3/6	10YR 4/2
HTN17087	HTN 9-B-2-1	Sierra Red: Sierra Variety	Dish	10R 4/6	10R 4/6	7.5YR 5/1
HTN17088	HTN 9-B-2-8	Sierra Red: Sierra Variety	Dish	2.5YR 4/8	2.5YR 4/8	10YR 7/2
HTN17089	HTN 9-B-3-1	Sierra Red: Sierra Variety	Bowl	10R 4/6	10R 4/6	10YR 5/1
HTN17090	HTN 9-B-3-3	Sierra Red: Sierra Variety	Bowl	10R 5/6	10R 4/6	10YR 6/1

				Munsell Values		
	Operation	**Type: Variety**	**Vessel Form**	**Exterior**	**Interior**	**Clean Break**
HTN17091	HTN 9-B-3-3	Sierra Red: Sierra Variety	Compound Form	10R 5/6	10R 4/6	10YR 5/2
HTN17092	HTN 9-B-3-5	Sierra Red: Sierra Variety	Jar	5YR 6/6	5YR 6/8	10YR 2/1
HTN17093	HTN 9-B-7-6	Sierra Red: Sierra Variety	Form Not Determined	2.5YR 4/6	2.5YR 3/6	10YR 3/1
HTN17094	HTN 20-3-7	Sierra Red: Sierra Variety	Jar	10R 5/6	10R 5/8	10YR 2/1
HTN17095	HTN 11-10-4	Sierra Red: Sierra Variety	Dish	10R 4/8	10R 5/6	10YR 3/1
HTN17096	HTN 11-10-4	Sierra Red: Sierra Variety	Dish	7.5R 4/6	7.5R 4/8	7.5YR 6/6
HTN17097	HTN 11-10-4	Sierra Red: Sierra Variety	Jar	10R 5/8	10R 5/8	7.5YR 6/4
HTN17098	HTN 11-11-5	Sierra Red: Sierra Variety	Bowl	10R 4/6	10R 4/6	2.5YR 4/6
HTN17099	HTN 11-11-5	Sierra Red: Sierra Variety	Dish	2.5YR 4/6	10R 4/8	7.5YR 7/6
HTN17100	HTN 11-12B-4	Sierra Red: Sierra Variety	Bowl	10R 5/8	10R 5/8	10YR 5/2
HTN17101	HTN 11-14-3	Sierra Red: Sierra Variety	Dish	10R 4/8	10R 5/8	7.5YR 5/6
HTN17102	HTN 11-15-3 (2)	Sierra Red: Sierra Variety	Dish	10R 3/6	10R 3/6	10YR 3/1
HTN17103	HTN 11-16-3	Sierra Red: Sierra Variety	Bowl	5YR 6/6	10R 4/8	10YR 4/1
HTN17104	HTN 11-2-3	Sierra Red: Sierra Variety	Dish	2.5YR 4/8	2.5YR 4/6	7.5YR 6/4
HTN17105	HTN 11-2-3	Sierra Red: Sierra Variety	Dish	5YR 4/6	5YR 4/6	7.5YR 6/6

	Operation	Type: Variety	Vessel Form	Munsell Values		
				Exterior	Interior	Clean Break
HTN17106	HTN 11-3-5	Sierra Red: Sierra Variety	Dish	10R 4/8	10R 4/8	2.5YR 6/6
HTN17109	HTN 11-4-5	Sierra Red: Sierra Variety	Dish	5YR 5/4	5YR 5/4	5YR 5/4
HTN17110	HTN 11-5-4	Sierra Red: Sierra Variety	Dish	10R 4/8	10R 4/8	10YR 4/2
HTN17111	HTN 11-6-5	Sierra Red: Sierra Variety	Dish	10YR 4/6	10R 3/6	7.5YR 4/1
HTN17112	HTN 11-6-6	Sierra Red: Sierra Variety	Dish	10R 5/8	2.5YR 5/6	5YR 5/4
HTN17113	HTN 11-6-6	Sierra Red: Sierra Variety	Dish	2.5YR 4/8	2.5YR 4/8	7.5YR 5/6
HTN17114	HTN 11-6-6	Sierra Red: Sierra Variety	Dish	10R 4/6	10R 4/6	7.5YR 4/2
HTN17115	HTN 11-6-6	Sierra Red: Sierra Variety	Dish	10R 3/4	10R 3/4	2.5YR 5/8
HTN17116	HTN 11-6-7	Sierra Red: Sierra Variety	Dish	10R 5/6	10R 5/6	7.5YR 3/1
HTN17117	HTN 11-6-7	Sierra Red: Sierra Variety	Dish	10R 4/8	10R 4/6	7.5YR 6/6
HTN17118	HTN 11-7-5	Sierra Red: Sierra Variety	Dish	10R 4/6	2.5YR 3/4	2.5YR 5/8
HTN17119	HTN 11-7-6	Sierra Red: Sierra Variety	Dish	10R 4/6	2.5YR 5/6	5YR 4/1
HTN17120	HTN 11-7-7	Sierra Red: Sierra Variety	Dish	2.5YR 5/6	7.5YR 6/6	10YR 4/3
HTN17121	HTN 11-7-7	Sierra Red: Sierra Variety	Dish	2.5YR 4/6	2.5YR 4/6	5YR 6/4
HTN17122	HTN 11-8-5	Sierra Red: Sierra Variety	Dish	2.5YR 4/6	2.5YR 4/6	10YR 6/3
HTN17123	HTN 11-8-5	Sierra Red: Sierra Variety	Dish	10R 4/6	10R 4/8	5YR 6/4

	Operation	Type: Variety	Vessel Form	Munsell Values		
				Exterior	Interior	Clean Break
HTN17126	HTN 11-8-7 (267-326cm)	Sierra Red: Sierra Variety	Dish	10R 4/6	10R 4/6	5YR 5/6
HTN17127	HTN 11-8-7 (267-326cm)	Sierra Red: Sierra Variety	Dish	10R 5/8	10R 4/8	7.5YR 6/6
HTN17128	HTN 11-8-7 (267-326cm)	Sierra Red: Sierra Variety	Dish	2.5YR 4/8	2.5YR 6/6	5YR 6/4
HTN17129	HTN 11-8-7 (267-326cm)	Sierra Red: Sierra Variety	Dish	10R 4/8	5YR 6/4	5YR 6/4
HTN17130	HTN 11-8-7 (267-326cm)	Sierra Red: Sierra Variety	Dish	2.5YR 5/8	2.5YR 5/6	7.5YR 6/4
HTN17131	HTN 11-8-7 (267-326cm)	Sierra Red: Sierra Variety	Dish	10R 5/6	10YR 3/2	5YR 5/4
HTN17132	HTN 11-8-7 (267-326cm)	Sierra Red: Sierra Variety	Dish	2.5YR 4/6	2.5YR 4/8	10YR 4/1
HTN17133	HTN 11-8-7 (267-326cm)	Sierra Red: Sierra Variety	Tecomate	10R 4/6	10R 4/6	2.5YR 5/6
HTN17134	HTN 11-8-7 (267-326cm)	Sierra Red: Sierra Variety	Dish	2.5YR 4/8	2.5YR 4/8	10YR 6/3
HTN17135	HTN 11-8-7 (267-326cm)	Sierra Red: Sierra Variety	Dish	10R 5/8	10R 5/6	10YR 5/4
HTN17136	HTN 11-8-8	Sierra Red: Sierra Variety	Dish	10R 4/6	10R 4/6	2.5YR 5/6
HTN17137	HTN 11-8-8	Sierra Red: Sierra Variety	Dish	2.5YR 5/6	10R 4/6	10YR 5/1
HTN17138	HTN 11-9-3	Sierra Red: Sierra Variety	Dish	10R 4/6	10R 5/6	7.5YR 7/6
HTN17139	HTN 11-9-3	Sierra Red: Sierra Variety	Dish	2.5YR 5/6	2.5YR 5/6	10YR 5/2
HTN17140	HTN 11-9-4	Sierra Red: Sierra Variety	Dish	10R 4/8	10R 4/6	5YR 6/6
HTN17141	HTN 11-9-4	Sierra Red: Sierra Variety	Dish	2.5YR 5/6	2.5YR 4/6	10YR 5/3

	Operation	Type: Variety	Vessel Form	Munsell Values		
				Exterior	Interior	Clean Break
HTN17142	HTN 2-29C-11-10	Sierra Red: Sierra Variety	Dish	10YR4/6	10YR 4/6	5YR 6/6
HTN17143	HTN 2-29C-11-16	Sierra Red: Sierra Variety	Dish	10R 4/6	2.5YR 4/6	7.5YR 6/4
HTN17144	HTN 2-29C-12-7	Sierra Red: Sierra Variety	Dish	10R 4/8	10R 4/6	2.5YR 4/6
HTN17145	HTN 11-8-6	Sierra Red: Sierra Variety	Dish	10R 4/6	10R 4/6	7.5YR 3/2
HTN17146	HTN 11-8-6	Pital Cream: Pital Variety	Dish	10YR 8/2	10YR 8/2	5YR 5/6
HTN17147	HTN 11-8-7 (216-267cm)	Pital Cream: Pital Variety	Jar	7.5YR 7/3	7.5YR 7/3	10YR 4/1
HTN17148	HTN 14-4-5	Pital Cream: Pital Variety	Dish	5YR 8/2	5YR 7/4	10YR 6/2
HTN17149	HTN 14-6-5	Pital Cream: Pital Variety	Dish	5YR 7/3	10YR 7/2	2.5Y 5/2
HTN17150	HTN 14-6-5	Pital Cream: Pital Variety	Dish	7.5YR 8/3	10YR 8/3	7.5YR 6/6
HTN17151	HTN 14-6-6	Pital Cream: Pital Variety	Dish	7.5YR 8/3	10YR 8/2	10YR 7/3
HTN17152	HTN 2-29A-6-19	Pital Cream: Pital Variety	Bowl	7.5YR 7/3	5YR 8/3	7.5YR 6/4
HTN17153	HTN 9-A-0	Pital Cream: Pital Variety	Dish	7.5YR 8/2	10YR 8/2	2.5YR 4/6
HTN17154	HTN 9-A-5-1	Pital Cream: Pital Variety	Jar	7.5YR 7/3	5YR 6/6	7.5YR 4/1
HTN17155	HTN 9-B-2-1	Pital Cream: Pital Variety	Dish	10YR 7/2	10YR 8/2	7.5YR 6/1
HTN17156	HTN 9-B-2-8	Flor Cream: Flor Variety	Vase	2.5YR 6/6	7.5YR 7/2	2.5YR 5/8
HTN17157	HTN 9-B-3-0	Flor Cream: Flor Variety	Dish	10YR 8/1	7.5YR 7/4	7.5YR 6/4

	Operation	Type: Variety	Vessel Form	Munsell Values		
				Exterior	Interior	Clean Break
HTN17158	HTN 9-B-3-1	Flor Cream: Flor Variety	Bowl	10YR 8/3	10YR 8/2	10YR 8/3
HTN17159	HTN 9-B-3-3	Flor Cream: Flor Variety	Bowl	10YR 8/2	10YR 7/4	10YR 7/1
HTN17160	HTN 9-B-3-6	Flor Cream: Flor Variety	Dish	10YR 8/1	10YR 8/1	2.5Y 7/2
HTN17161	HTN 9-B-4	Flor Cream: Flor Variety	Dish	7.5YR 7/3	7.5YR 7/3	2.5Y 6/1
HTN17162	HTN 9-B-6	Flor Cream: Flor Variety	Bowl	2.5Y 8/1	2.5Y 8/1	2.5Y 7/1
HTN17163	HTN 11-10-5	Flor Cream: Flor Variety	Dish	2.5YR 5/6	2.5YR 5/6	10YR 6/3
HTN17164	HTN 11-14-3	Flor Cream: Flor Variety	Bowl	7.5YR 6/4	5YR 6/4	7.5YR 5/4
HTN17165	HTN 11-14-3	Flor Cream: Flor Variety	Bowl	10YR 7/3	7.5YR 6/6	10YR 6/2
HTN17166	HTN 11-17-3	Flor Cream: Flor Variety	Dish	5YR 7/1	7.5YR 7/6	10YR 8/3
HTN17167	HTN 11-6-6	Flor Cream: Flor Variety	Jar	5YR 6/6	5YR 6/6	7.5YR 6/6
HTN17168	HTN 11-6-7	Flor Cream: Flor Variety	Dish	7.5YR 6.4	7.5YR 6/2	5YR 5/4
HTN17169	HTN 11-7-7	Flor Cream: Flor Variety	Dish	7.5YR 6/3	7.5YR 7/3	10YR 5/4
HTN17170	HTN 11-8-7 (267-326cm)	Flor Cream: Flor Variety	Bowl	7.5YR 6/4	7.5YR 6/6	2.5YR 4/2
HTN17171	HTN 11-9-4	Flor Cream: Flor Variety	Bowl	7.5YR 7/3	7.5YR 6/4	10YR 6/4
HTN17172	HTN 20-3-6	Flor Cream: Flor Variety	Jar	7.5YR 7/4	7.5YR 7/4	10YR 4/1
HTN17173	HTN 20-3-6	Flor Cream: Flor Variety	Bowl	5YR 6/4	7.5YR 7/3	7.5YR 7/6

	Operation	Type: Variety	Vessel Form	Munsell Values		
				Exterior	Interior	Clean Break
HTN17175	HTN 2-29C-11-10	Flor Cream: Flor Variety	Bowl	5YR 7/6	7.5YR 6/6	2.5YR 6/4
HTN17176	HTN 2-29C-11-10	Flor Cream: Flor Variety	Dish	10YR 4/1	7.5YR 5/3	2.5YR 4/6
HTN17177	HTN 2-29C-11-10	Flor Cream: Flor Variety	Bowl	7.5YR 6/2	10YR 6/2	7.5YR 7/4
HTN17178	HTN 2-29C-11-10	Flor Cream: Flor Variety	Tecomate	7.5YR 7/4	7.5YR 7/4	2.5Y 3/1
HTN17179	HTN 2-29C-11-14	Flor Cream: Flor Variety	Dish	7.5YR 6/2	7.5YR 5/1	5YR 5/4
HTN17180	HTN 2-29C-11-14	Chunhinta Black: Chunhinta Variety	Form Not Determined	-	-	7.5YR 4/2
HTN17181	HTN 2-29C-11-14	Chunhinta Black: Chunhinta Variety	Form Not Determined	-	-	2.5YR 5/6
HTN17182	HTN 2-29C-11-15	Chunhinta Black: Chunhinta Variety	Form Not Determined	-	-	10YR 6/1
HTN17183	HTN 2-29C-11-15	Chunhinta Black: Chunhinta Variety	Form Not Determined	-	-	5YR 4/6
HTN17184	HTN 2-29C-11-15	Chunhinta Black: Chunhinta Variety	Form Not Determined	-	-	10YR 6/3
HTN17185	HTN 2-29C-11-15	Chunhinta Black: Chunhinta Variety	Form Not Determined	-	-	10YR 5/2
HTN17186	HTN 2-29C-11-15	Chunhinta Black: Chunhinta Variety	Form Not Determined	-	-	10YR 4/1
HTN17187	HTN 2-29C-11-17	Chunhinta Black: Chunhinta Variety	Dish	-	-	10YR 4/2
HTN17188	HTN 2-29C-11-5	Chunhinta Black: Chunhinta Variety	Dish	-	-	10YR 4/2
HTN17189	HTN 2-29C-11-5	Chunhinta Black: Chunhinta Variety	Dish	-	-	7.YR 6/2
HTN17190	HTN 2-29C-11-5	Chunhinta Black: Chunhinta Variety	Tecomate	-	-	10YR 2/2

	Operation	Type: Variety	Vessel Form	Munsell Values		
				Exterior	Interior	Clean Break
HTN17191	HTN 2-29C-11-5	Chunhinta Black: Chunhinta Variety	Vase	-	-	2.5Y 4/8
HTN17192	HTN 2-29C-11-6	Chunhinta Black: Chunhinta Variety	Jar	-	-	10YR 5/2
HTN17193	HTN 2-29C-11-6	Chunhinta Black: Chunhinta Variety	Jar	-	-	7.5YR 5/3
HTN17194	HTN 2-29C-11-7	Chunhinta Black: Chunhinta Variety	Dish	-	-	2.5Y 5/1
HTN17195	HTN 2-29C-11-7	Chunhinta Black: Chunhinta Variety	Dish	-	-	10YR 5/2
HTN17196	HTN 2-29C-12-10	Chunhinta Black: Chunhinta Variety	Dish	-	-	5YR 6/3
HTN17197	HTN 2-29C-12-11	Chunhinta Black: Chunhinta Variety	Dish	-	-	5YR 5/6
HTN17198	HTN 2-29C-12-11	Chunhinta Black: Chunhinta Variety	Jar	-	-	2.5YR 4/8
HTN17199	HTN 2-29C-12-11	Chunhinta Black: Chunhinta Variety	Dish	-	-	2.5YR 4/6
HTN17200	HTN 2-29C-12-11	Chunhinta Black: Chunhinta Variety	Dish	-	-	7.5YR 4/2
HTN17201	HTN 2-29C-12-11	Chunhinta Black: Chunhinta Variety	Dish	-	-	2.5YR 5/6
HTN17202	HTN 2-29C-12-7	Chunhinta Black: Chunhinta Variety	Dish	-	-	5YR 5/6
HTN17203	HTN 2-29C-12-7	Chunhinta Black: Chunhinta Variety	Dish	-	-	5YR 5/6
HTN17204	HTN 2-29C-12-7	Chunhinta Black: Chunhinta Variety	Jar	-	-	10R 4/6
HTN17205	HTN 2-29C-12-7	Chunhinta Black: Chunhinta Variety	Jar	-	-	2.5YR 4/6
HTN17206	HTN 2-29C-12-7	Chunhinta Black: Chunhinta Variety	Jar	-	-	10R 5/6

	Operation	Type: Variety	Vessel Form	Munsell Values		
				Exterior	Interior	Clean Break
HTN17207	HTN 2-29C-12-7	Chunhinta Black: Chunhinta Variety	Dish	-	-	10YR 4/1
HTN17208	HTN 2-29C-12-7	Chunhinta Black: Chunhinta Variety	Dish	-	-	2.5YR 5/4
HTN17209	HTN 2-29C-12-7	Chunhinta Black: Chunhinta Variety	Dish	-	-	2.5YR 5/6
HTN17210	HTN 2-29C-12-7	Chunhinta Black: Chunhinta Variety	Dish	-	-	10YR 3/1
HTN17211	HTN 2-29C-12-8	Chunhinta Black: Chunhinta Variety	Dish	-	-	10YR 6/1
HTN17212	HTN 2-29C-12-8	Chunhinta Black: Chunhinta Variety	Jar	-	-	7.5YR 2.5/1
HTN17213	HTN 2-29C-12-8	Chunhinta Black: Chunhinta Variety	Jar	-	-	10YR 4/3
HTN17214	HTN 2-29C-12-8	Chunhinta Black: Chunhinta Variety	Bowl	-	-	10YR 3/1
HTN17215	HTN 2-29C-12-8	Chunhinta Black: Chunhinta Variety	Vase	-	-	10YR 5/1
HTN17216	HTN 2-29C-12-9	Chunhinta Black: Chunhinta Variety	Tecomate	-	-	10YR 6/1
HTN17217	HTN 2-29C-12-9	Chunhinta Black: Chunhinta Variety	Bowl	-	-	10YR 5/1
HTN17218	HTN 2-29C-12-9	Chunhinta Black: Chunhinta Variety	Form Not Determined	-	-	10R 4/6
HTN17219	HTN 2-29C-12-9	Chunhinta Black: Chunhinta Variety	Form Not Determined	-	-	10YR 3/1
HTN17220	HTN 2-29C-12-9	Chunhinta Black: Chunhinta Variety	Form Not Determined	-	-	10YR 2/1
HTN17221	HTN 2-29C-12-9	Chunhinta Black: Chunhinta Variety	Dish	-	-	10YR 4/1
HTN17222	HTN 2-29C-12-9	Chunhinta Black: Chunhinta Variety	Dish	-	-	5YR 3/3

	Operation	Type: Variety	Vessel Form	Munsell Values		
				Exterior	Interior	Clean Break
HTN17223	HTN 11-3A-7	Chunhinta Black: Chunhinta Variety	Dish	-	-	10R 6/6
HTN17224	HTN 11-6-6	Chunhinta Black: Chunhinta Variety	Dish	-	-	2.5YR 6/8
HTN17225	HTN 11-8-6	Chunhinta Black: Chunhinta Variety	Dish	-	-	10YR 3/1
HTN17226	HTN 11-8-7 (216-267cm)	Chunhinta Black: Chunhinta Variety	Dish	-	-	5YR 5/6
HTN17227	HTN 11-9-5	Chunhinta Black: Chunhinta Variety	Dish	-	-	7.5YR 5/2
HTN17228	HTN 11-8-6	Chunhinta Black: Chunhinta Variety	Bowl	-	-	10YR 3/1
HTN17229	HTN 11-3A-7	Chunhinta Black: Chunhinta Variety	Jar	-	-	10YR 4/2
HTN17230	HTN 11-3A-7	Chunhinta Black: Chunhinta Variety	Bowl	-	-	7.5YR 5/4
HTN17231	HTN 11-8-7 (216-267cm)	Chunhinta Black: Chunhinta Variety	Jar	-	-	7.5YR 6/1
HTN17232	HTN 11-8-7 (216-267cm)	Chunhinta Black: Chunhinta Variety	Dish	-	-	5YR 4/4
HTN17233	HTN 11-9-5	Chunhinta Black: Chunhinta Variety	Dish	-	-	10YR 5/3
HTN17234	HTN 14-4-5	Chunhinta Black: Chunhinta Variety	Dish	-	-	10YR 7/1
HTN17235	HTN 14-4-5	Chunhinta Black: Chunhinta Variety	Jar	-	-	2.5Y 3/2
HTN17236	HTN 14-4-5	Chunhinta Black: Chunhinta Variety	Dish	-	-	2.5Y 3/1
HTN17237	HTN 14-4-5	Chunhinta Black: Chunhinta Variety	Jar	-	-	10YR 2/1
HTN17238	HTN 14-4-5	Chunhinta Black: Chunhinta Variety	Dish	-	-	10YR 5/3

	Operation	Type: Variety	Vessel Form	Munsell Values		
				Exterior	Interior	Clean Break
HTN17239	HTN 14-4-5	Chunhinta Black: Chunhinta Variety	Dish	-	-	10YR 3/2
HTN17240	HTN 14-6-5	Chunhinta Black: Chunhinta Variety	Dish	-	-	10YR 5/3
HTN17241	HTN 14-6-5	Chunhinta Black: Chunhinta Variety	Dish	-	-	10YR 6/4
HTN17242	HTN 14-6-5	Chunhinta Black: Chunhinta Variety	Dish	-	-	7.5YR 4/3
HTN17243	HTN 14-6-6	Chunhinta Black: Chunhinta Variety	Dish	-	-	10YR 6/2
HTN17244	HTN 14-6-6	Chunhinta Black: Chunhinta Variety	Dish	-	-	7.5YR 7/4
HTN17245	HTN 14-6-6	Chunhinta Black: Chunhinta Variety	Dish	-	-	10YR 5/4
HTN17246	HTN 14-6-6	Chunhinta Black: Chunhinta Variety	Dish	-	-	7.5YR 6/6
HTN17247	HTN 14-12-4	Chunhinta Black: Chunhinta Variety	Dish	-	-	5YR 5/6
HTN17248	HTN 14-12-4	Chunhinta Black: Chunhinta Variety	Jar	-	-	10YR 5/1
HTN17249	HTN 14-12-4	Chunhinta Black: Chunhinta Variety	Dish	-	-	7.5YR 6/4
HTN17250	HTN 14-12-4	Chunhinta Black: Chunhinta Variety	Dish	-	-	7.5YR 5/3
HTN17251	HTN 14-12-4	Chunhinta Black: Chunhinta Variety	Dish	-	-	5YR 5/4
HTN17252	HTN 14-12-4	Chunhinta Black: Chunhinta Variety	Dish	-	-	10YR 3/1
HTN17253	HTN 14-12-4	Chunhinta Black: Chunhinta Variety	Dish	-	-	10YR 4/2
HTN17254	HTN 14-12-4 (2)	Chunhinta Black: Chunhinta Variety	Dish	-	-	10YR 4/1

				Munsell Values		
	Operation	**Type: Variety**	**Vessel Form**	**Exterior**	**Interior**	**Clean Break**
HTN17255	HTN 14-12-4 (2)	Chunhinta Black: Chunhinta Variety	Dish	-	-	10YR 6/4
HTN17256	HTN 14-12-4 (2)	Chunhinta Black: Chunhinta Variety	Dish	-	-	10YR 3/1
HTN17257	HTN 20-3A-8	Chunhinta Black: Chunhinta Variety	Dish	-	-	10YR 2/1
HTN17258	HTN 25-1-3	Chunhinta Black: Chunhinta Variety	Dish	-	-	7.5YR 5/1
HTN17259	HTN 20-3A-9	Chunhinta Black: Chunhinta Variety	Jar	-	-	2.5Y 4/1
HTN17260	HTn 2-29A-6-17	Chunhinta Black: Chunhinta Variety	Jar	-	-	7.5YR 5/1
HTN17261	HTN 9-A-10	Chunhinta Black: Chunhinta Variety	Jar	-	-	2.5Y 3/2
HTN17262	HTN 9-A-10	Chunhinta Black: Chunhinta Variety	Jar	-	-	2.5YR 4/6
HTN17263	HTN 9-A-1-1	Chunhinta Black: Chunhinta Variety	Dish	-	-	7.5YR 6/6
HTN17264	HTN 9-A-6-1	Chunhinta Black: Chunhinta Variety	Dish	-	-	10YR 5/3
HTN17265	HTN 9-A-9	Polvero Black: Polvero Variety	Dish	-	-	10YR 6/4
HTN17266	HTN 9-B-2-2	Polvero Black: Polvero Variety	Jar	-	-	10YR 3/1
HTN17267	HTN 9-B-2-6	Polvero Black: Polvero Variety	Compound Form	-	-	10YR 5/3
HTN17268	HTN 9-B-2-7	Polvero Black: Polvero Variety	Dish	-	-	10YR 4/1
HTN17269	HTN 9-B-2-7	Polvero Black: Polvero Variety	Bowl	-	-	10YR 3/1
HTN17270	HTN 9-B-2-8	Polvero Black: Polvero Variety	Dish	-	-	7.5YR 5/4

	Operation	Type: Variety	Vessel Form	Munsell Values		
				Exterior	Interior	Clean Break
HTN17271	HTN 9-B-2-8	Polvero Black: Polvero Variety	Dish	-	-	10YR 7/4
HTN17272	HTN 9-B-3-1	Polvero Black: Polvero Variety	Compound Form	-	-	2.5YR 5/4
HTN17273	HTN 9-B-3-1	Polvero Black: Polvero Variety	Compound Form	-	-	2.5Y 3/1
HTN17274	HTN 9-B-3-5	Polvero Black: Polvero Variety	Bowl	-	-	10YR 6/3
HTN17275	HTN 9-B-3-6	Polvero Black: Polvero Variety	Bowl	-	-	10YR 5/2
HTN17276	HTN 9-B-3-6	Polvero Black: Polvero Variety	Bowl	-	-	10YR 4/2
HTN17277	HTN 9-B-3-7	Polvero Black: Polvero Variety	Bowl	-	-	10YR 5/1
HTN17278	HTN 9-B-4	Polvero Black: Polvero Variety	Jar	-	-	7.5YR 5/3
HTN17279	HTN 9-B-4	Polvero Black: Polvero Variety	Dish	-	-	5YR 5/6
HTN17280	HTN 11-2-3	Polvero Black: Polvero Variety	Bowl	-	-	2.5Y 5/1
HTN17281	HTN 11-2-8	Polvero Black: Polvero Variety	Jar	-	-	2.5Y 4/1
HTN17282	HTN 11-2-8	Polvero Black: Polvero Variety	Dish	-	-	2.5Y 3/1
HTN17283	HTN 11-3-5	Polvero Black: Polvero Variety	Compound Form	-	-	10YR 4/1
HTN17284	HTN 11-5-4	Polvero Black: Polvero Variety	Dish	-	-	10YR 4/2
HTN17285	HTN 11-5-5	Polvero Black: Polvero Variety	Jar	-	-	7.5YR 6/6
HTN17286	HTN 11-6-6	Polvero Black: Polvero Variety	Dish	-	-	10YR 5/2

				Munsell Values		
	Operation	Type: Variety	Vessel Form	Exterior	Interior	Clean Break
HTN17287	HTN 11-6-7	Polvero Black: Polvero Variety	Dish	-	-	5YR 6/4
HTN17288	HTN 11-6-7	Polvero Black: Polvero Variety	Jar	-	-	7.5YR 5/4
HTN17289	HTN 11-7-6	Polvero Black: Polvero Variety	Dish	-	-	5YR 5/3
HTN17290	HTN 11-8-3	Polvero Black: Polvero Variety	Dish	-	-	7.5YR 5/6
HTN17291	HTN 11-8-4	Polvero Black: Polvero Variety	Bowl	-	-	2.5YR 4/4
HTN17292	HTN 11-8-5	Polvero Black: Polvero Variety	Dish	-	-	5YR 4/4
HTN17293	HTN 11-8-7 (267-326cm)	Polvero Black: Polvero Variety	Bowl	-	-	10YR 4/2
HTN17294	HTN 11-8-7 (267-326cm)	Polvero Black: Polvero Variety	Jar	-	-	7.5YR 5/3
HTN17295	HTN 11-8-7 (267-326cm)	Polvero Black: Polvero Variety	Jar	-	-	2.5YR 4/6
HTN17296	HTN 11-8-7 (267-326cm)	Polvero Black: Polvero Variety	Jar	-	-	2.5YR 5/6
HTN17297	HTN 11-8-7 (267-326cm)	Polvero Black: Polvero Variety	Dish	-	-	10YR 5/4
HTN17298	HTN 11-9-4	Polvero Black: Polvero Variety	Dish	-	-	10YR 4/3
HTN17299	HTN 11-12A-4	Polvero Black: Polvero Variety	Jar	-	-	10YR 3/1
HTN17300	HTN 11-14-3	Polvero Black: Polvero Variety	Jar	-	-	7.5YR 5/3
HTN17301	HTN 11-14-3	Polvero Black: Polvero Variety	Jar	-	-	7.5YR 5/3
HTN17302	HTN 11-14-3	Polvero Black: Polvero Variety	Dish	-	-	7.5YR 4/2

	Operation	Type: Variety	Vessel Form	Munsell Values		
				Exterior	Interior	Clean Break
HTN17303	HTN 11-15-3	Polvero Black: Polvero Variety	Jar	-	-	10YR 2/1
HTN17304	HTN 11-15-3	Polvero Black: Polvero Variety	Dish	-	-	2.5Y 4/2
HTN17305	HTN 11-17-3	Polvero Black: Polvero Variety	Jar	-	-	10YR 5/4
HTN17306	HTN 14-5-3	Polvero Black: Polvero Variety	Jar	-	-	10YR 5/2
HTN17307	HTN 14-6-4	Polvero Black: Polvero Variety	Jar	-	-	10YR 6/2
HTN17308	HTN 20-4-3	Polvero Black: Polvero Variety	Form Not Determined	-	-	10YR 6/3
HTN17309	HTN 20-3-7	Polvero Black: Polvero Variety	Dish	-	-	10YR 7/3
HTN17310	HTN 24-4-2	Polvero Black: Polvero Variety	Bowl	-	-	10YR 5/2
HTN17311	Group A	Polvero Black: Polvero Variety	Dish	-	-	10YR 6/4
HTN17312	Group A	Polvero Black: Polvero Variety	Dish	-	-	7.5YR 6/4
HTN17313	Holtun West	Polvero Black: Polvero Variety	Dish	-	-	10YR 4/2
HTN17314	Holtun West	Polvero Black: Polvero Variety	Dish	-	-	10YR 4/1
HTN17315	Holtun West	Polvero Black: Polvero Variety	Dish	-	-	10YR 4/3

REFERENCES

Adams, Richard E.

1971 The Ceramics of Altar de Sacrificios. *Papers of the Peabody Museum of Archaeology and Ethnology* 63:1. Harvard University, Cambridge.

Aimers, Jim J., Don J. Farthing, and Aaron N. Shugar

2012 Handheld XRF Analysis of Maya Ceramics: A Pilot Study Presenting Issues Related to Quantification and Calibration. In *Handheld XRF for Art and Archaeology*, edited by Aaron N. Shugar and Jennifer L. Mass, pp. 423-448. Studies in Archaeological Science, No 3, Patrick Degryse, general editor, Leuven University Press, Leuven.

al-Saad, Ziad

2002 Chemical Composition and Manufacturing Technology of a Collection of Various Types of Islamic Glazes Excavated from Jordan. *Journal of Archaeological Science* 29:803-810

Barclay, Katherine

2002 *Scientific Analysis of Archaeological Ceramics: A Handbook of Resources*. Oxbow Books, Oxford.

Bezur, Anikó, and Francesca Casadio

2012 The Analysis of Porcelain Using Handheld and Portable X-Ray Fluorescence Spectrometers. In *Handheld XRF for Art and Archaeology*, edited by Aaron N. Shugar and Jennifer L. Mass, pp. 249-313. Studies in Archaeological Science, No 3, Patrick Degryse, general editor, Leuven University Press, Leuven.

Bill, Cassandra R.

2013 Types and Traditions, Spheres and Systems: A Consideration of Analytic Constructs and Concepts in the Classification and Interpretation of Maya Ceramics. In *Ancient Maya Pottery*, edited by James John Aimers, pp. 29-45. University Press of Florida, Gainesville.

Brouwer, Peter

2010 *Theory of XRF Getting Acquainted with the Principals*. PANalytical, Lelyweg.

Bruker

2013 Use of XRF for Mudrock and Ceramic Measurements. Electronic document, save date January 16, 2013.

n.d. XRF Data Differences: Quantitative, Semi-Quantitative, and Qualitative Data. Web page, https://www.bruker.com/products/x-ray-diffraction-and-elemental-analysis/handheld-xrf/xrf-data-primer-quantitative-semi-quantitative-qualitative.html, accessed January 23, 2019.

Callaghan, Michael G., and Nina Neivens de Estrada

2016 *The Ceramic Sequence of the Holmul Region*. Anthropological Papers of the University of Arizona No. 77. University of Arizona Press, Tucson.

Callaghan, Michael G., Daniel E. Pierce, Bridgette Kovacevich, and Michael D. Glascock

2017 Chemical Paste Characterization of Late Middle Preclassic-period Ceramics from Holtun, Guatemala and its Implications for Production and Exchange. *Journal of Archaeological Science: Reports* 12:334-345.

Cardona, Karla, Michael Callaghan, and Brigitte Kovacevich (editors)

2015 *Informe Preliminar de Investigaciones Arqueologicas en Holtun, Guatemala*: *Temporada 2014*. Instituto de Antropologia e Historia, Guatemala.

2016 *Informe Preliminar de Investigaciones Arqueologicas en Holtun, Guatemala*: *Temporada 2015*. Instituto de Antropologia e Historia, Guatemala.

2017 *Informe Preliminar de Investigaciones Arqueologicas en Holtun, Guatemala*: *Temporada 2016*. Instituto de Antropologia e Historia, Guatemala.

2018 *Informe Preliminar de Investigaciones Arqueologicas en Holtun, Guatemala*: *Temporada 2017*. Instituto de Antropologia e Historia, Guatemala.

Cecil, Leslie G.

2013 Slips, Styles, and Trading Patterns: A Postclassic Perspective from Central Petén, Guatemala. In *Ancient Maya Pottery: Classification, Analysis, and Interpretation*, edited by James John Aimers, pp. 185-202. University of Florida Press, Gainesville.

Cecil, Leslie G., and Hector Neff

2006 Postclassic Maya Slips and Paints and Their Relationship to Socio-Political Groups in El Petén, Guatemala. *Journal of Archaeological Science* 33:1482-1491.

Chilton, Elizabeth S.

1998 The Cultural Origins of Technical Choice: Unraveling Algonquian and Iroquoian Ceramic Traditions in the Northeast. In Stark, M. T. (ed.), *The Archaeology of Social Boundaries*, Smithsonian Institution Press, Washington, DC, pp. 132–160.

Dietler, Michael, and Ingrid Herbich.

1989 Tich matek: The Technology of Luo Pottery Production and the Definition of Ceramic Style. *World Archaeology* 21: 148-164.

Drake, Lee

2018 Depth of Analysis. Electronic document, http://www.xrf.guru/Concepts/DepthOfAnalysis/index.html, accessed November 12, 2018.

Ferguson, Jeffery R., Scott Van Keuren, and Shilo Bender

2015 Rapid Qualitative Compositional Analysis of Ceramic Paints. *Journal of Archaeological Science: Reports* 3:321-327.

Fialko, Vilma

2002 *Documentación del Arte Escultórico y Pictórico de la Acrópolis Tríadica de Holtun, Peten, Guatemala.* Proyecto Protección de Sitios Arqueológicos de Peten (PRONAT-TRIÁNGULO-DEMOPRE). IDAEH, Guatemala.

Forsyth, Donald W.

1989 The Ceramics of El Mirador, Peten, Guatemala. El Mirador Series, Part 4. *Papers of the New World Archaeological Foundation* 63. Brigham Young University, Provo.

Gifford, James C.

1976 Prehistoric Pottery Analysis and the Ceramics of Barton Ramie in the Belize Valley. *Memoirs of the Peabody Museum of Archaeology and Ethnology* 18. Harvard University, Cambridge.

Glascock, Michael D.

1992 Characterization of Archaeological Ceramics at MURR by Neutron Activation Analysis and Multivariate Statistics. In *Chemical Characterization of Ceramics Pastes in Archaeology*, edited by Hector Neff, pp. 11-26. Prehistory Press, Madison.

Guzmán Piedrasanta, Rodrigo

2016 Mapa arqueológico de Holtun. In *Proyecto arqueológico Holtun informe: no. 6, temporada 2016*, edited by Karla J. Cardona Caravantes, Michael Callaghan, and Brigitte Kovacevich, pp. 32-65. Proyecto Arqueológico Holtun, Guatemala City, Guatemala.

Hall, E. T.

1960 X-Ray Fluorescent Analysis Applied to Archaeology. *Archaeometry* 3(1):29-37.

Hunt, Alice M. W., and Robert J. Speakman

2015 Portable XRF Analysis of Archaeological Sediments and Ceramics. *Journal of Archaeological Science* 53:1-13.

Kosakowsky, Laura J.

1987 Preclassic Maya Pottery at Cuello, Belize. *Anthropological Papers* No. 47. University of Arizona Press, Tucson. Liritzis, Ioannis, and Nikolaos Zachaias

2012 Portable XRF of Archaeological Artifacts: Current Research, Potential and Limitations. In *X-Ray Fluorescence Spectrometry (XRF) in Geoarchaeology*, edited by M. Steven Shackley, pp. 109-142. Springer, New York.

Kovacevich, Brigitte, Karla Cardona, Michael Callaghan, and Melvin Rodrigo Guzman (editors)

2014 *Informe Preliminar de Investigaciones Arqueologicas en Holtun, Guatemala*: *Temporada 2012*. Instituto de Antropologia e Historia, Guatemala.

Kovacevich, Brigitte, Patricia Rivera Castillo, Michael Callaghan, and Melvin Rodrigo Guzman (editors)

2011 *Informe Preliminar de Investigaciones Arqueologicas en Holtun, Guatemala*: *Temporada 2010*. Instituto de Antropologia e Historia, Guatemala.

2012 *Informe Preliminar de Investigaciones Arqueologicas en Holtun, Guatemala*: *Temporada 2011*. Instituto de Antropologia e Historia, Guatemala.

McGlinchey, Chris

2012 Handheld XRF for the Examination of Paintings: Proper Use and Limitations. In *Handheld XRF for Art and Archaeology*, edited by Aaron N. Shugar and Jennifer L. Mass, pp. 131-159. Studies in Archaeological Science, No 3, Patrick Degryse, general editor, Leuven University Press, Leuven.

Molera, Judit, Mario Vendrell-Saz, and Josefina Pérez-Arantegui

2001 Chemical and Textural Characterization of Tin Glazes in Islamic Ceramics from Eastern Spain. *Journal of Archaeological Science* 28:331-340.

Neff, Hector

2003 Analysis of Mesoamerican Plumbate Pottery Surfaces by Laser Ablation Inductively Coupled Plasma-Mass Spectrometry (LA-ICP-MS). *Journal of Archaeological Science* 30:21-35.

Neff, Hector, Barabara Voorhies, and Federico Paredes Umaña

2012 Handheld XRF Elemental Analysis of Archaeological Sediments: Some Examples from Mesoamerica, In *Handheld XRF for Art and Archaeology*, edited by Aaron N. Shugar and Jennifer L. Mass, pp. 379-399. Studies in Archaeological Science, No 3, Patrick Degryse, general editor, Leuven University Press, Leuven.

Ortega-Feliu, Inés, Blanca Gómez-Tubío, Yasmina Cárceres, and Miguel Ángel Respaldiza

2018 Characterization of Glaze Ceramics from the Archaeological Site of La Alcazaba, Almería (Spain). *Microchemical Journal* 138:72-81

Ponciano, Erick M.

1995 "Recientes descubrimientos en el departamento de Peten: Sitio Arqueológico Holtun, Aldea La Máquina, Flores." En VIII Simposio de Investigaciones Arqueológicas en Guatemala 1994, editado por J.P. Laporte y H. Escobedo. MUNAE. Guatemala.

Rauschenberg, Bradford L.

2005 Carl Eisenberg's Introduction of Tin-Glazed Ceramics to Salem, North Carolina, and Evidence for Early Tin-Glaze Production Elsewhere in North America. *Journal of Early Southern Decorative Arts* 31:45-103.

Rice, Prudence M.

1981 Evolution of Specialized Pottery Production: A Trial Model. *Current Anthropology* 22(3):219-240.

1987 *Pottery Analysis: A Sourcebook.* Chicago: University of Chicago Press.

2013 Type-Variety: What Works and What Doesn't. In *Ancient Maya Pottery*, edited by James John Aimers, pp. 11-28. University Press of Florida, Gainesville.

Sabloff, Jeremy E.

1975 Ceramics. In *Excavations at Seibal, Department of Peten, Guatemala.* Memoirs of the Peabody Museum of Archaeology and Ethnology. Vol. 13(2). Harvard University, Cambridge.

Schlotz, Reinhold, and Stefan and Uhlig

2006 *Introduction to X-Ray Fluorescence (XRF).* Bruker AXS, Inc., Madison.

Shackley, M. Steven

2012a X-Ray Fluorescence Spectrometry in Twenty-First Century Archaeology. In *X-Ray Fluorescence Spectrometry (XRF) in Geoarchaeology*, edited by M. Steven Shackley, pp. 1-6. Springer, New York.

2012b An Introduction to X-Ray Fluorescence (XRF) Analysis in Archaeology. In *X-Ray Fluorescence Spectrometry (XRF) in Geoarchaeology*, edited by M. Steven Shackley, pp. 7-44. Springer, New York.

Shugar, Aaron N., and Jennifer L. Mass

2012 Introduction. In *Handheld XRF for Art and Archaeology*, edited by Aaron N. Shugar and Jennifer L. Mass, pp. 17-36. Studies in Archaeological Science, No 3, Patrick Degryse, general editor, Leuven University Press, Leuven.

Shepard, Anna O.

1956 *Ceramics for the Archaeologist*. Carnegie Institute of Washington, Washington D.C.

Speakman, Robert J., Nicole C Little, Darrell Creel, Myles R. Miller, and Javier G. Iñañez

2011 Sourcing Ceramics with Portable XRF Spectrometers? A Comparison with INAA Using Mimbres Pottery from the American Southwest. *Journal of Archaeological Science* 38:3483-3496.

Speakman, Scott A.

n.d. Using the Bruker Tracer III-SD Handheld X-Ray Fluorescence Spectrometer using PC Software for Data Collection. Electronic document, http://prism.mit.edu/xray/oldsite/Bruker%20XRF%20SOP.pdf, accessed November 12, 2018.

Willis, James P. and Andrew R. Duncan

2008 *Understanding XRF Spectrometry: Basic Concepts and Instrumentation.* PANalytical, Lelyweg.